Highway Traffic State Estimation Per Lane in the Presence of Connected Vehicles

Nikolaos Bekiaris-Liberis, Claudio Roncoli, and Markos Papageorgiou

Abstract

A model-based traffic state estimation approach is developed for per-lane density estimation as well as on-ramp and off-ramp flows estimation for highways in presence of connected vehicles. Three are the basic ingredients of the developed estimation scheme: (1) a data-driven version of the conservation-of-vehicles equation (in its time- and space-discretized form); (2) the utilization of position and speed information from connected vehicles' reports, as well as total flow measurements obtained from a minimum number (sufficient for the observability of the model) of fixed detectors, such as, for example, at the main entry and exit of a given highway stretch; and (3) the employment of a standard Kalman filter. Furthermore, necessary and sufficient conditions for the (strong) structural observability of the introduced model are established (properties, which are rarely studied in the literature on traffic estimation), which yield the fixed detectors requirements needed for the proper operation of the developed estimation scheme. The performance of the estimation scheme is evaluated for various penetration rates of connected vehicles utilizing real microscopic traffic data collected within the Next Generation SIMulation (NGSIM) program. It is shown that the estimation performance is satisfactory, in terms of a suitable metric, even for low penetration rates of connected vehicles. The sensitivity of the estimation performance to variations of the model parameters (two in total) is also quantified, and it is shown that, overall, the estimation scheme is little sensitive to the model parameters.

I. Introduction

A. Motivation

Lane-specific highway traffic management has considerable potential in traffic flow optimization. As it is well-known since the early 1990s [56], the presence of connected and automated vehicles could play a key role in the exploitation of this potential [14], [15], [24], [36], [37]. More specifically, significant throughput improvements may be achieved via appropriate real-time lane assignment strategies. Prominent approaches are mandatory lane policies and lane advices, which can be achieved via lane-changing control strategies, such as, for example, [4], [13], [19], [23], [41], [42], [43], [44], [45], [46], or lane-dependent

N. Bekiaris-Liberis and M. Papageorgiou are with the Department of Production Engineering & Management, Technical University of Crete, Chania, Greece, 73100. Email addresses: nikos.bekiaris@dssl.tuc.gr and markos@dssl.tuc.gr.

C. Roncoli is with the Department of Built Environment, School of Engineering, Aalto University, 02150 Espoo, Finland. Email address: claudio.roncoli@aalto.fi.

variable speed limits [10], [21], [61]. The operation of lane-based highway traffic control calls for real-time information reflecting the current traffic conditions per lane.

B. Literature Review

The effectiveness of lane-based traffic management strategies largely depends on the quality and accuracy of traffic monitoring at a lane level. Numerous traffic state estimation methodologies exist, amply based on the presence of connected vehicles, which, however, do not distinguish the density values among different lanes, such as, for example, [2], [5], [9], [11], [12], [17], [18], [35], [39], [40], [47], [48], [49], [50], [53], [55], [57], [58], [59], [60]. The existing works dealing with the problem of traffic state estimation per lane are rare and, in addition, they employ almost exclusively measurements coming from fixed detectors [6], [7], [20], [51], [52]; with the notable exception of [62], where a somewhat heuristic, model-based approach is developed using Lagrangian coordinates, in which measurements stemming from connected vehicles' reports are utilized. It is worth highlighting that in [62] the knowledge of a fundamental diagram is required, which is not needed in the present paper.

C. Contribution

In this paper, we address the problem of per-lane density estimation as well as ramp flow estimation in highways, via the development of a model-based estimation approach, which relies largely on the presence of connected vehicles. We denote connected vehicles all vehicles that are capable of reporting information (i.e., position and speed) to an infrastructure-based system, which may be achieved via different technologies and communication paradigms. A basic scenario may simply consist of vehicles equipped with a GPS (Global Positioning System) and a system for mobile communication. However, more complex scenarios, for example scenarios that incorporate communication among vehicles or between vehicles and roadside units, are also possible.

The basic ingredients of the developed estimation scheme are: (1) a data-driven version of the conservation-of-vehicles equation (in its time- and space-discretized form); (2) the utilization of position and speed information from connected vehicles' reports, as well as total flow measurements obtained from a minimum number (sufficient for the observability of the model) of fixed detectors, such as, for example, at the entry and exit of a given highway stretch; and (3) the employment of a standard Kalman filter.

In addition, we study the observability properties of the introduced model. Specifically, we provide sufficient and necessary conditions for the structural observability as well as the strong structural observability, see, for example, [16], [25], [26], [27], [38], of our model; it should be noted that observability properties are rarely studied in the literature on traffic estimation. As a result, we characterize the fixed detectors configuration that guarantee the proper operation of the developed estimation scheme. The stability properties of the estimator are also discussed.

The performance of the estimation scheme is evaluated for various penetration rates of connected vehicles utilizing real microscopic traffic data collected within the Next Generation SIMulation (NGSIM) program, see, for example, [28], [29]. It is shown that the estimation performance is satisfactory, in terms of a suitable metric, even for low penetration rates of connected vehicles. The sensitivity of the estimation performance to variations of the model parameters (two in total) is also quantified and it is shown that, overall, the estimation scheme is little sensitive to the model parameters.

D. Organization

In Section II the model for the density dynamics and the estimation scheme are introduced. In Section III the structural observability properties of the developed model are studied and the stability properties of the estimator are discussed. In Section IV the performance of the estimation scheme is validated via the employment of NGSIM data.

E. Notation and Definitions

a) Notation: We adopt the notation from [38] (see also, e.g., [25], [27]):

- A structured matrix $\mathcal{A}$, i.e., a matrix with certain elements being either fixed zeros or free nonzero parameters, is called a pattern. We say that a matrix A is of pattern $\mathcal{A}$ if the structure of its zero and nonzero elements is the same with $\mathcal{A}$ for all times.
- The graph $\mathcal{G}(\mathcal{A}, \mathcal{C})$, where $\mathcal{A}$ and $\mathcal{C}$ are of dimension $n \times n$ and $r \times n$, respectively, has vertices $\{1, \ldots, n+r\}$ and there is a (directed) edge from the vertex x to the vertex w if the element (w, x) of $(\mathcal{A}, \mathcal{C})$ is a nonzero parameter. In this case, x is a predecessor of w, and w is a successor of x. For any set V of vertices, $\text{Pre}(V)$ denotes the set of predecessors of V, namely, the set of all vertices with a directed edge to some vertex in V. The set $\text{Post}(V)$ denotes the set of successors of V, namely, the set of all vertices with a directed edge from some vertex of V.

- Vertices $\{1, \ldots, n\}$ represent the states of the underlined dynamical system and are called "state" vertices, whereas vertices $\{n, \ldots, n+r\}$ represent those specific states for which noisy measurements are available, and are called "output" vertices.
- A vertex is called non-accessible if there exists no path (i.e., a sequence of directed edges connecting certain distinct vertices) from any output vertex to that vertex. A graph is said to contain a dilation if there exists a set V of state vertices such that the cardinality of the set $\text{Pre}\,(V)$ is strictly smaller than the cardinality of the set V.

b) Definitions: Consider a linear discrete-time system of the form

$$x(k+1) = A(k)x(k) + B(k)u(k) \tag{1}$$

$$y(k) = C(k)x(k) + D(k)u(k), \tag{2}$$

where $x \in \mathbb{R}^n$ is state, $u \in \mathbb{R}^M$ is input, $y \in \mathbb{R}^r$ is output, and $k = 0, 1, \ldots$ is the discrete time. We adopt the following definitions, see, e.g., [1], [27], [38]:

- The pair of matrices (A, C) is called observable on $[k_0, k_0 + M^*]$ if and only if for all initial conditions $x(k_0) \in \mathbb{R}^n$ and for all inputs $u : [k_0, k_0 + M^*] \to \mathbb{R}^r$, one can uniquely determine $x(k_0)$ from the information $\{(u(k), y(k))\,|k \in [k_0, k_0 + M^*]\}$.

We assume now that matrices A and C are of pattern $\mathcal{A}$ and $\mathcal{C}$, respectively.

- The system is strongly structurally observable if *for any* numerical realization of the structured matrices $\mathcal{A}$ and $\mathcal{C}$, the corresponding systems are observable in the sense of the formal definition above.
- The system is (weakly) structurally observable if *there exist* numerical realizations of the structured matrices $\mathcal{A}$ and $\mathcal{C}$, such that the corresponding systems are observable in the sense of the formal definition above.

The conditions that must be satisfied for strong or (weak) structural observability are provided in the Appendix for the convenience of the reader.

II. Per Lane Traffic Density Estimation Using a Data-Driven Model

A. General Set-Up

We consider highway stretches consisting of M lanes, indexed by $j = 1, \ldots, M$, subdivided into N segments, indexed by $i = 1, \ldots, N$. We define a cell (i, j) to be the highway part that corresponds to lane j of segment i. The length of each segment is denoted by Δ_i, $i = 1, \ldots, N$.

The following variables are repeatedly used in the paper:

- Average speed $\left[\frac{\text{km}}{\text{h}}\right]$ of vehicles in cell (i, j), denoted by $v_{i,j}$, for $i = 1, \ldots, N$ and $j = 1, \ldots, M$.
- Total traffic density $\left[\frac{\text{veh}}{\text{km}}\right]$ at cell (i, j), denoted by $\rho_{i,j}$, for $i = 1, \ldots, N$ and $j = 1, \ldots, M$.
- Total longitudinal inflow $\left[\frac{\text{veh}}{\text{h}}\right]$ of cell $(i+1, j)$, denoted by $q_{i,j}$, for $i = 0, \ldots, N-1$ and $j = 1, \ldots, M$.
- Total on-ramp flow $\left[\frac{\text{veh}}{\text{h}}\right]$ entering at cell (i, j), denoted by $r_{i,j}$, for $i = 1, \ldots, N$ and $j = 1, \ldots, M$.
- Total off-ramp flow $\left[\frac{\text{veh}}{\text{h}}\right]$ exiting from cell (i, j), denoted by $s_{i,j}$, for $i = 1, \ldots, N$ and $j = 1, \ldots, M$.
- Total lateral flow $\left[\frac{\text{veh}}{\text{h}}\right]$ at segment i that enters lane j_2 from lane j_1, denoted by $L_{i,j_1 \to j_2}$, for $i = 1, \ldots, N$, $j_1 = 1, \ldots, M$, and $j_2 = j_1 \pm 1$.

B. Available Information from Connected Vehicles' Reports

The data-driven model, which is presented in the next subsection, requires the availability of the following measurements:

- Average speed of connected vehicles at cell (i, j), denoted by $v^{\text{c}}_{i,j}$, for $i = 1, \ldots, N$ and $j = 1, \ldots, M$.
- Density of connected vehicles at cell (i, j), denoted by $\rho^{\text{c}}_{i,j}$, for $i = 1, \ldots, N$ and $j = 1, \ldots, M$.
- Lateral flow of connected vehicles at segment i that enters lane j_2 from lane j_1, denoted by $L^{\text{c}}_{i,j_1 \to j_2}$, for $i = 1, \ldots, N$, $j_1 = 1, \ldots, M$, and $j_2 = j_1 \pm 1$.

Notice that average speeds, densities, and lateral flows of connected vehicles may be obtained based on position and speed reports (see also Section IV-A).

C. Model Description for the Density Dynamics

The conservation equation yields the following model for the density dynamics in each cell (i, j)

$$\begin{aligned} \rho_{i,j}(k+1) \;=\; & \rho_{i,j}(k) + \frac{T}{\Delta_i}\left(q_{i-1,j}(k) - q_{i,j}(k) + L_{i,j-1\to j}(k) + L_{i,j+1\to j}(k)\right. \\ & \left. - L_{i,j\to j-1}(k) - L_{i,j\to j+1}(k) + r_{i,j}(k) - s_{i,j}(k)\right), \end{aligned} \tag{3}$$

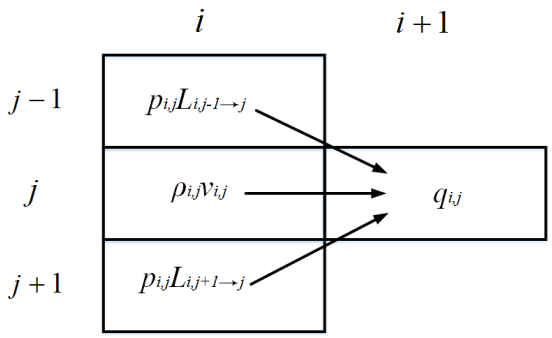

Fig. 1. Model of the exiting longitudinal flow from cell (i, j) as described in (4). It consists of a well-established term of the form $\rho_{i,j} v_{i,j}$, to the contribution of the cell density, and of additional terms, which are multiplied by a certain percentage p, due to the contribution of "diagonal" lateral flows.

where T denotes the time discretization step. For convenience[1], we assume $r_{i,j} \equiv s_{i,j} \equiv 0$ for all i and $1 \leq j \leq M-1$, where M denotes the right-most lane (assuming right-hand traffic); also, we have $L_{i,j_1 \to j_2} \equiv 0$ if either j_1 or j_2 equals zero or $M+1$. We note that the inflows at the entry of the highway, namely, $q_{0,j}$, for all $j = 1, \ldots, M$, are treated as measured inputs to system (3).

We employ the following relation for the total flows (see Fig. 1)

$$\begin{aligned} q_{i,j}(k) &= v_{i,j}(k)\rho_{i,j}(k) + p_{i,j} L_{i,j-1 \to j}(k) + p_{i,j} L_{i,j+1 \to j}(k) + \bar{p}_{i,j} r_{i,j}(k), \\ &\quad \text{for } i = 1, \ldots, N \text{ and } j = 1, \ldots, M, \end{aligned} \tag{4}$$

where $p_{i,j} \in [0, 1]$, $\bar{p}_{i,j} \in [0, 1]$, for $i = 1, \ldots, N$ and $j = 1, \ldots, M$, are real numbers that indicate the percentages of "diagonal" lateral movements, including the lateral flows from an on-ramp "lane", for each specific cell. While the choice of the first term in (4) is well-known (see, e.g., [31]), the motivation for the choice of the rest three terms in (4) is less obvious. This choice is guided from the fact that at locations where strong lateral flows are observed, such as, for example, at cells where an on-ramp is located or at segments that feature lane-drops, a significant amount of the lateral flow may appear close to the end of those cells (e.g., in the former case, where the acceleration lane ends). As a result, the flow modeling may be more accurately described when considering that a percentage of lateral and on-ramp flows actually acts as additional exiting longitudinal flow. This conclusion is confirmed by the estimation results obtained using NGSIM data, in which we observe that an estimation bias may appear if all $p_{i,j}$ and $\bar{p}_{i,j}$ values are set to zero. In fact, this formulation is also employed in other works, see, e.g., [22].

[1]Although, for convenience we assume that there are no on-ramps or off-ramps on the left-most lane, the model could be easily adapted to incorporate such cases (which are, however, not common in practice). Moreover, the model could be also easily adapted to incorporate the case where the number of lanes is not the same for all segments, as is the case, for example, when there are lane-drops or lane-gains.

The percentages $p_{i,j}$ and $\bar{p}_{i,j}$ are viewed as tuning parameters. In the most general case, these percentages may be different to each other. For example, one may expect that two percentages $\bar{p}_{i,j}$ that correspond to two respective on-ramps with different acceleration lane lengths are different to each other. However, it was observed in the testing with NGSIM data in Section IV, that the estimation performance is not really affected if the percentage values are chosen equal to zero for all segments, except those featuring strong lateral flows, such as segments with on-ramps or lane drops. This significantly reduces the number of the parameters that need to be specified[2].

For the lateral flows, we employ the following relation

$$L_{i,j_1\to j_2}(k) = \frac{L^{\mathrm{c}}_{i,j_1\to j_2}(k)}{\rho^{\mathrm{c}}_{i,j_1}(k)}\rho_{i,j_1}(k), \quad \text{for } i = 1,\dots,N,\ j_1 = 1,\dots,M, \text{ and } j_2 = j_1 \pm 1. \tag{5}$$

Equation (5) is based on the reasonable assumption that the proportion of lane-changing connected vehicles is equal to the proportion of all lane-changing vehicles. We consider this as a reasonable assumption also for various scenarios that include automated (and controlled) vehicles. In fact, in case there is no strict infrastructure-based need for lane changing, we expect rather low lane-changing flows, and, in fact, we could even utterly ignore lane changing and still obtain reasonable estimation results (see Section IV). For this reason, it is not of crucial importance to measure accurately and account for this (very low) proportion. On the other hand, in case there is a strict infrastructure-based need for lane changing (such as, for example, near ramps or a lane-drop), then we may have stronger lateral flows that need to be measured. In such a case, despite automated vehicles may have a different microscopic lane-changing behavior, they have not much of other choice than to change lane; these lane-changes may happen slightly earlier or later than for manual vehicles, but roughly in proportions which are similar to what manual vehicles also need to perform. Therefore, despite this assumption may not be always exactly valid, we expect that at macroscopic level this may produce only a local bias in the lateral flows, which does not affect significantly the resulting traffic estimates. Furthermore, in case one would observe that this bias produces unacceptable deterioration of the estimation performance, the proposed methodology may be extended to account explicitly for the bias, via definition of a modified model (5) for lateral flows.

This allows one to quantify the total lateral movements from a cell using (5), namely by scaling the

[2]For instance, in the testing with NGSIM data, only one percentage value is needed to be non-zero (and thus, to be tuned), namely, the value that corresponds to the cell where an on-ramp is located.

lateral movements of connected vehicles with the inverse of the percentage of connected vehicles in that cell. The accuracy of formulation (5) is tested in the estimation results of Section IV. Note that, for analysis, the densities of connected vehicles are assumed to be strictly positive, whereas, in practice, the problem of the possible division, in relation (5) with zero at some time instants, may be resolved by employing a heuristic procedure (see Section IV-A).

Plugging (4), (5) into (3), we re-write the total density dynamics for all (i, j) as

$$\begin{aligned}\rho_{i,j}(k+1) &= \left(1-\frac{T}{\Delta_i}v_{i,j}(k)-\frac{T}{\Delta_i}\frac{L^{\mathrm{c}}_{i,j\to j-1}(k)}{\rho^{\mathrm{c}}_{i,j}(k)}-\frac{T}{\Delta_i}\frac{L^{\mathrm{c}}_{i,j\to j+1}(k)}{\rho^{\mathrm{c}}_{i,j}(k)}\right)\rho_{i,j}(k)+\frac{T}{\Delta_i}v_{i-1,j}(k)\rho_{i-1,j}(k)\\ &+(1-p_{i,j})\frac{T}{\Delta_i}\frac{L^{\mathrm{c}}_{i,j-1\to j}(k)}{\rho^{\mathrm{c}}_{i,j-1}(k)}\rho_{i,j-1}(k)+(1-p_{i,j})\frac{T}{\Delta_i}\frac{L^{\mathrm{c}}_{i,j+1\to j}(k)}{\rho^{\mathrm{c}}_{i,j+1}(k)}\rho_{i,j+1}(k)\\ &+p_{i-1,j}\frac{T}{\Delta_i}\frac{L^{\mathrm{c}}_{i-1,j-1\to j}(k)}{\rho^{\mathrm{c}}_{i-1,j-1}(k)}\rho_{i-1,j-1}(k)+p_{i-1,j}\frac{T}{\Delta_i}\frac{L^{\mathrm{c}}_{i-1,j+1\to j}(k)}{\rho^{\mathrm{c}}_{i-1,j+1}(k)}\rho_{i-1,j+1}(k)\\ &+(1-\bar{p}_{i,j})\frac{T}{\Delta_i}r_{i,j}(k)+\bar{p}_{i-1,j}\frac{T}{\Delta_i}r_{i-1,j}(k)-\frac{T}{\Delta_i}s_{i,j}(k),\end{aligned} \tag{6}$$

where, according to the conventions adopted in Section II-C, for all i and $j=1$, the terms $\frac{L^{\mathrm{c}}_{i,j\to j-1}(k)}{\rho^{\mathrm{c}}_{i,j}(k)}\rho_{i,j}(k)$, $\frac{L^{\mathrm{c}}_{i,j-1\to j}(k)}{\rho^{\mathrm{c}}_{i,j-1}(k)}\rho_{i,j-1}(k)$, and $\frac{L^{\mathrm{c}}_{i-1,j-1\to j}(k)}{\rho^{\mathrm{c}}_{i-1,j-1}(k)}\rho_{i-1,j-1}(k)$ should be set to zero; for all i and $j=M$, the terms $\frac{L^{\mathrm{c}}_{i,j\to j+1}(k)}{\rho^{\mathrm{c}}_{i,j}(k)}\rho_{i,j}(k)$, $\frac{L^{\mathrm{c}}_{i,j+1\to j}(k)}{\rho^{\mathrm{c}}_{i,j+1}(k)}\rho_{i,j+1}(k)$, and $\frac{L^{\mathrm{c}}_{i-1,j+1\to j}(k)}{\rho^{\mathrm{c}}_{i-1,j+1}(k)}\rho_{i-1,j+1}(k)$ should be set to zero; and for all j and $i=1$, the terms $\frac{L^{\mathrm{c}}_{i-1,j-1\to j}(k)}{\rho^{\mathrm{c}}_{i-1,j-1}(k)}\rho_{i-1,j-1}(k)$, $\frac{L^{\mathrm{c}}_{i-1,j+1\to j}(k)}{\rho^{\mathrm{c}}_{i-1,j+1}(k)}\rho_{i-1,j+1}(k)$, and $r_{i-1,j}(k)$ should be set to zero.

To enable also the estimation of unmeasured on-ramp and off-ramp flows within the highway stretch, we will adopt, as usual in absence of a descriptive dynamic model, a random walk for the quantities to be estimated. The deterministic parts of such models (to be eventually augmented with additive zero-mean, white Gaussian noise) for on-ramp and off-ramp flow estimation, respectively, read

$$r_{i,M}(k+1) = r_{i,M}(k) \tag{7}$$

$$s_{i,M}(k+1) = s_{i,M}(k). \tag{8}$$

We write next compactly the overall system (6)–(8). For this, we define first the vector x as follows

$$x=\left(\rho_{1,1},\cdots,\rho_{N,1},\cdots,\rho_{1,M}\cdots,\rho_{N,M},r_{1,M},\cdots,r_{N,M},s_{1,M},\cdots,s_{N,M}\right)^{\mathrm{T}}. \tag{9}$$

The average speed of connected vehicles is representative of the average cell speed, as motivated in [5] and justified with real data and in microscopic simulation in [40] and [12], respectively, even for

connected-vehicle penetrations as low as 2%. Thus the unmeasured cell speeds $v_{i,j}$ may be replaced by the corresponding measured speeds $v^{\mathrm{c}}_{i,j}$; and, using (9), we re-write (6)–(8) in a compact form as

$$x(k+1) \;\; = \;\; A\left(v^{\mathrm{c}}(k), L^{\mathrm{c}}(k), \rho^{\mathrm{c}}(k)\right) x(k) + Bu(k), \tag{10}$$

where v^{c}, L^{c}, and ρ^{c} denote vectors that incorporate all average cell speeds of connected vehicles $v^{\mathrm{c}}_{i,j}$, lateral flows of connected vehicles $L^{\mathrm{c}}_{i,j_1 \to j_2}$, and densities of connected vehicles $\rho^{\mathrm{c}}_{i,j}$, respectively, while u denotes the vector of inflows at the highway entrance, namely, $u = (q_{0,1}, \cdots, q_{0,M})^{\mathrm{T}}$, $A \in \mathbb{R}^{(N\times M+2N)\times(N\times M+2N)}$, and $B \in \mathbb{R}^{(N\times M+2N)\times M}$.

Together with (10) we associate an output vector y, which holds all mainstream total flows that are measured by corresponding mainstream fixed detectors and, as follows from (4), (5), is given by

$$y(k) = C\left(v^{\mathrm{c}}(k), L^{\mathrm{c}}(k), \rho^{\mathrm{c}}(k)\right) x(k), \tag{11}$$

where $C \in \mathbb{R}^{(M+l_r+l_s-1)\times(N\times M+2N)}$, with l_r and l_s being the number of on-ramps and off-ramps, respectively. The minimum number of rows of C equals $M + l_r + l_s - 1$ in order for system (10), (11) to be observable (see Section III), which is true when the total flows at the last segment of every lane as well as the total flows of lane M at every segment that is anywhere between two consecutive unmeasured ramps, are measured. Yet, any additional available mainstream measurement could be incorporated in (11) in order to improve the estimation performance. Note that we assume $2N$ ramp flows. In the case where there are less on-ramp or off-ramp flows, the dimension of the matrices A, B, and C are reduced accordingly.

The total flow measurements may be replaced by corresponding density measurements when, for instance, occupancy detectors are available instead of flow detectors and are used to deduce corresponding density values. In this case, the corresponding entries of the C matrix in (11) would simply be equal to one. Moreover, when there are both speed and flow detectors in a cell, the entries of the C matrix that correspond to average cell speeds obtained from connected vehicles' reports may be replaced by the total average speed measured by the detector.

D. Per Lane Total Density Estimation Employing a Kalman Filter

We employ next a standard Kalman filter [3] along the lines of [5] (see also [12], [40]). The estimation equations are given by

$$\begin{aligned}
\hat{x}(k+1) &= A\left(v^{\mathrm{c}}(k), L^{\mathrm{c}}(k), \rho^{\mathrm{c}}(k)\right)\hat{x}(k) + Bu(k) \\
&\quad + A\left(v^{\mathrm{c}}(k), L^{\mathrm{c}}(k), \rho^{\mathrm{c}}(k)\right) K(k)\left(z(k) - C\left(v^{\mathrm{c}}(k), L^{\mathrm{c}}(k), \rho^{\mathrm{c}}(k)\right)\hat{x}(k)\right) \qquad (12) \\
K(k) &= P(k)C\left(v^{\mathrm{c}}(k), L^{\mathrm{c}}(k), \rho^{\mathrm{c}}(k)\right)^{\mathrm{T}} \\
&\quad \times \Big(C\left(v^{\mathrm{c}}(k), L^{\mathrm{c}}(k), \rho^{\mathrm{c}}(k)\right) P(k) C\left(v^{\mathrm{c}}(k), L^{\mathrm{c}}(k), \rho^{\mathrm{c}}(k)\right)^{\mathrm{T}} + R\Big)^{-1} \qquad (13) \\
P(k+1) &= A\left(v^{\mathrm{c}}(k), L^{\mathrm{c}}(k), \rho^{\mathrm{c}}(k)\right)\left(I - K(k)C\left(v^{\mathrm{c}}(k), L^{\mathrm{c}}(k), \rho^{\mathrm{c}}(k)\right)\right) \\
&\quad \times P(k) A\left(v^{\mathrm{c}}(k), L^{\mathrm{c}}(k), \rho^{\mathrm{c}}(k)\right)^{\mathrm{T}} + Q, \qquad (14)
\end{aligned}$$

where $\hat{x}$ denotes the estimate of vector x defined in (10), z is a noisy version of the measurement y defined in (11), $R = R^{\mathrm{T}} > 0$, $Q = Q^{\mathrm{T}} > 0$, and $P(k_0) = P(k_0)^{\mathrm{T}} > 0$. Note that, in the ideal case in which there is additive, zero-mean Gaussian white noise in equations (10) and (11), respectively, R and Q represent the (ideally known) covariance matrices of the measurement and process noise, respectively. In the ideal case in which $x(k_0)$ is a Gaussian random variable, the initial conditions of the filter (12)–(14), namely, $\hat{x}(k_0)$ and $P(k_0)$ represent the mean and auto covariance matrix of $x(k_0)$, respectively. More details on the meaning of each of the tuning parameter $\hat{x}(k_0), P(k_0)$, Q, and R can be found in [3], [5].

In summary, in order to run the estimation scheme (12)–(14) the following measurements are needed (see also Section III for more details):

- Total flows exiting from the last cell of every lane, which are the M elements of the output vector y as well as total flows entering into the first segment of every lane, which are comprised in the input vector u.
- Total exiting flows of lane M at every cell that is anywhere between two consecutive unmeasured ramps, which are the $l_r + l_s - 1$ elements of the output vector y.
- Speeds, lateral flows, and densities of connected vehicles, which are comprised in the vectors v^{c}, L^{c}, and ρ^{c}, respectively, and may be obtained by speed and position reports stemming from connected vehicles.

III. Observability of the Model and Stability of the Estimation Scheme

A. Observability: Physical Implications

For the benefit of readers that may not be familiar with the concept of observability, we provide next some physically oriented implications of the formal definitions of Section I-E (see, e.g., [1], [27]).

In less rigorous terms, the observability property of a system guarantees that the dynamic evolution of its internal states (i.e., the states that are not directly measured) may be extracted (observed) by measuring only some specific states (or, more generally, some outputs of the system). Thus, the study of observability of a system is useful since it provides the necessary sensor requirements, which guarantee that all internal sates may be reconstructed by measuring only certain outputs. For example, in a traffic system, studying the observability for a given highway stretch one can derive the locations at which the mainstream fixed flow detectors should be placed, in order to guarantee that the densities in all cells may be reconstructed by measuring the flow only at these particular locations. In particular, as far as real-time traffic state estimation is concerned, observability is a property that guarantees that the state of system (10), (11), i.e., all cell densities, can be reproduced, in real time in an unbiased way from the available measurements by use of the Kalman filter (12)–(14).

B. The Concept of Structural Observability

Observability of a system is usually studied employing certain algebraic conditions, see, e.g., [1] (see also paragraphs *d)–f)* in the Appendix). However, for systems with a very large number of states or very large output matrices or for time-varying systems (as in our case) it is difficult to formally check these conditions. For this reason, as an alternative, graph-theoretic approaches are adopted, which study the observability properties of a system by merely looking into its structure, see, e.g., [16], [25], [26], [27], [38]. In addition, the study of the *structural* observability properties of a system is useful in that one can determine under which measurement configurations a system is observable, by investigating the structure of the zero and non-zero elements of the A and C matrices. Depending on which specific notion is adopted, structural observability may be a sufficient or necessary condition for observability (see paragraphs a) and b) below and the definitions in Section I-E).

Here we focus on two different notions of structural observability, namely the *strong* structural observ-

ability and the (*weak*)[3] structural observability whose (informal) definitions can be found in Section I-E. We provide next some of the implications of the two structural observability properties on observability, and consequently, on traffic state estimation.

a) Strong Structural Observability: The strong structural observability property guarantees that "no matter what" values the non-zero system matrix elements may take, the system remains observable. Thus, clearly, strong structural observability is sufficient for observability.

b) (Weak) Structural Observability: Is a neccasary condition for observability. The (weak) structural observability concept, in fact, provides a physically intuitive way to the study of observability which, in *practice*, typically implies indeed system observability. The reason is that the loss of observability of a (weakly) structurally observable system may happen only in some "pathological" cases when the elements of the A and C matrices accidentally happen to satisfy some specific conditions, see, e.g., [25], [27], [38]. Thus, in practice, as it is also suggested from the estimation results in Section IV, (weak) structural observability implies in the rule the proper operation of an estimation scheme as the one presented here. It should be also noted that, since (weak) structural observability is a weaker property than strong structural observability, one may expect that a smaller number of sensors may be required to guarantee (weak) structural observability than strong structural observability.

C. Structural Assumptions for the Considered Traffic Models

We consider systems of the form (10), (11) with the patterns $\mathcal{A}$ and $\mathcal{C}$ under the assumptions that for all (i,j) it holds that

$$v^{\mathrm{c}}_{i,j}(k) \neq 0, \quad \text{for all } k \geq 0 \tag{15}$$

$$1 - \frac{T}{\Delta_i} v^{\mathrm{c}}_{i,j}(k) - \frac{T}{\Delta_i} \frac{L^{\mathrm{c}}_{i,j\to j-1}(k)}{\rho^{\mathrm{c}}_{i,j}(k)} - \frac{T}{\Delta_i} \frac{L^{\mathrm{c}}_{i,j\to j+1}(k)}{\rho^{\mathrm{c}}_{i,j}(k)} \neq 0, \quad \text{for all } k \geq 0. \tag{16}$$

Both conditions (15), (16) are satisfied when for all (i,j) it holds that

$$0 < v^{\mathrm{c}}_{i,j}(k) < \frac{\Delta_i}{T} - \frac{L^{\mathrm{c}}_{i,j\to j-1}(k)}{\rho^{\mathrm{c}}_{i,j}(k)} - \frac{L^{\mathrm{c}}_{i,j\to j+1}(k)}{\rho^{\mathrm{c}}_{i,j}(k)}, \quad \text{for all } k \geq 0. \tag{17}$$

The right-hand side of inequality (17), in the case of zero lateral flows of connected vehicles (e.g., in the case of one-lane highway), is satisfied when the traffic model respects the so-called Courant-Friedrichs-Lewy (CFL) condition [8] (which must anyhow hold for stable discrete traffic flow models). The left-hand

[3]Note that, in the literature, the weak structural observability property comes usually under the name "structural observability". However, here, we use the name "(weak) structural observability" so no confusion arises.

side of inequality (17) is satisfied when at least one connected vehicle is not completely stopped within a cell. In practice, the satisfaction of this requirement may be handled via opportune heuristic rules, such as, for example, the utilization of a moving average of a certain number of past, non-zero speed values (see also Section IV).

D. Traffic Models Under Study

In the following structural observability study we consider subsequently the following four basic models derived from the general model (10), (11); each sub-model turns out to have different structural observability properties:

I. One-lane highway stretch with N segments ($\equiv$ cells), where all percentage values $\bar{p}_{i,j}$ for diagonal on-ramp[4] flows are set to zero (which is equivalent to the non-lane-based estimation scheme for a highway stretch considered in [5]).

II. General three-lane highway stretch[5] where all percentage values $p_{i,j}$ and $\bar{p}_{i,j}$ are set equal to zero, for both diagonal lateral and on-ramp flows, whereas the lateral flows of connected vehicles may or may not be zero.

III. General three-lane highway stretch.

IV. One-lane highway stretch where the percentage values $\bar{p}_{i,j}$ for diagonal on-ramp flows may be non-zero.

In the study of (weak) structural observability we consider in addition the following two models:

V. Model I where matrix A is replaced by $\frac{1}{T}(A - I)$, which can be viewed as an approximation of the continuous-time version of Model I (where the time derivative is approximated by a forward finite difference formula).

VI. Model III where matrix A is replaced by $\frac{1}{T}(A - I)$, which can be viewed as an approximation of the continuous-time version of Model III (where the time derivative is approximated by a forward finite difference formula).

The motivation for studying these additional models will be explained later (see Section III-F).

[4]Note that for simplicity of presentation we consider the case in which all unmeasured ramps are on-ramps. The same arguments apply in the case where there are unmeasured off-ramps as well since the off-ramp flow dynamics are identical to the on-ramp flow dynamics.

[5]For simplicity of presentation we consider specifically a three-lane highway stretch.

Note that, as it is already mentioned in Section II, the inflows at the main entry of each lane of the considered highway stretch are modeled as arbitrary, but measured, inputs. Consequently, in the subsequent structural observability studies, it is tacitly presumed that at the main entry of each lane of the considered highway stretch there is a fixed flow detector. Yet, all the specific models and the following observability analysis could be adapted to the case where some inflows are not directly measured. For example, one could model the unmeasured inflows with random walk equations, which could be treated similarly to unmeasured on-ramp flows that are considered in the following subsections. Finally, for simplicity of presentation we consider the case in which none of the on-ramp flows is directly measured.

E. Strong Structural Observability of Lane-Based Highway Traffic

We establish the following claims for each of the models I, II, III, and IV:

1. Model I is strongly structurally observable if and only if : i) total flow fixed detectors are placed at the main exit of the considered highway stretch; and ii) total flow fixed detectors are placed at every segment immediately upstream of a segment with an on-ramp[6].
2. Model II is strongly structurally observable if and only if: i) total flow fixed detectors are placed at the main exit in each lane of the considered highway stretch; and ii) total flow fixed detectors are placed at every segment immediately upstream of a segment with an on-ramp.
3. Model III is not strongly structurally observable under the measurement configuration i) and ii) of Claim 2.
4. Model IV is not strongly structurally observable under the measurement configuration i) and ii) of Claim 1.

In order to establish Claims 1–4 we employ the results from [38] under the structural assumptions of Section III-C.

a) Claim 1: We start by constructing the graph $\mathcal{G}\left(\mathcal{A}^{\mathrm{T}}, \mathcal{C}^{\mathrm{T}}\right)$, shown in Fig. 2, for Model I. Employing Corollary IV.2 from [38] (see also [16]), it follows that the highway stretch with one lane is strongly structurally observable on $[k_0, k_0 + N + m]$, for any $k_0 \geq 0$, where m denotes the total number of on-ramps (hence, that every system of pattern $(\mathcal{A}, \mathcal{C})$ is observable on $[k_0, k_0 + N + m]$) if and only if condition

[6]This may also be proved (as far as the sufficiency part is concerned) as in [5] employing an algebraic approach and utilizing the classical definition of observability.

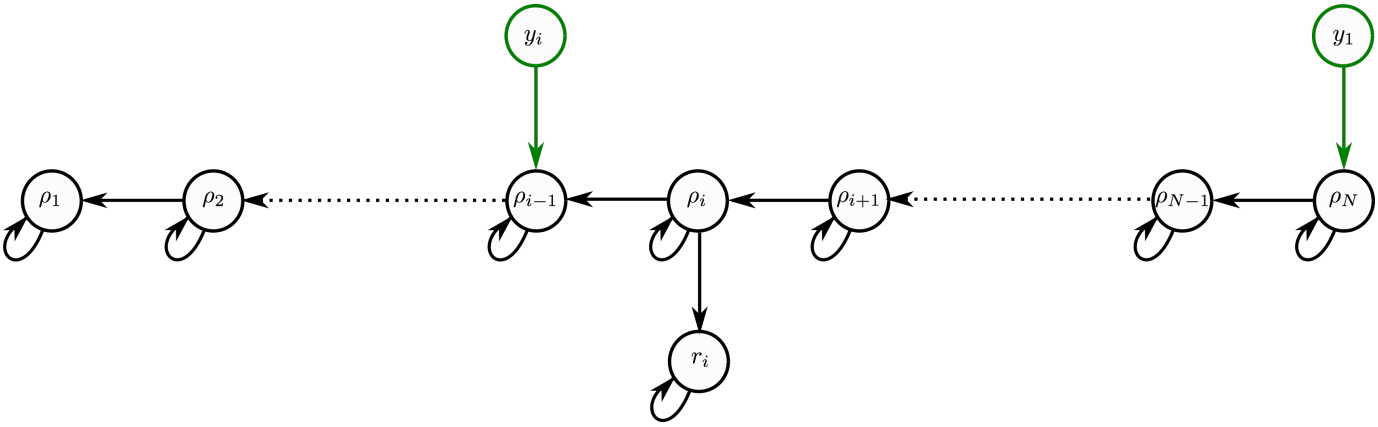

Fig. 2. The graph $\mathcal{G}\left(\mathcal{A}^{\mathrm{T}}, \mathcal{C}^{\mathrm{T}}\right)$ for patterns $\mathcal{A}$ and $\mathcal{C}$ that include matrices A and C, respectively, of system (10), (11), for the case of a simple one-lane highway stretch with N segments (Model I).

$G_0 \cap G_1$ is satisfied. For the reader's convenience, conditions G_0 and G_1 can be found in the Appendix.

A sufficient requirement for condition G_0 to be satisfied is that the total flow at the exit of the considered highway stretch is measured, or, more generally, that there is an output vertex y_1 as shown in Fig. 2. To see this, first observe from Fig. 2 that for every subset $S \subseteq \{\rho_1, \ldots, \rho_N\}$ it holds that $S \cap \text{Post}\left(\{\rho_{j+1}\}\right) = \{\rho_j\}$, where ρ_j corresponds to the vertex with the maximum index that belongs to S with $\rho_j \equiv y_1$ when $j = N + 1$. Moreover, for every such subset S that also includes vertices of the form r_i, it holds that $S \cap \text{Post}\left(\{r_i\}\right) = \{r_i\}$.

We next show that a sufficient requirement for condition G_1 to hold is that, simultaneously, mainstream, total flow fixed detectors are placed at every segment immediately upstream of a segment with an on-ramp as well as at the exit of the stretch. We first note that the requirement of condition G_1, that $V \subseteq \text{Pre}\left(V\right)$, is indeed satisfied for any subset $V \subseteq \{\rho_1, \ldots, \rho_N, r_1, \ldots, r_m\}$, since, as it is observed from Fig. 2, for every vertex there is a directed edge from that vertex to itself. We employ next the same argument to the proof of satisfaction of condition G_0, namely that for every subset $S \subseteq \{\rho_1, \ldots, \rho_N\}$ it holds that $S \cap \text{Post}\left(\{\rho_{j+1}\}\right) = \{\rho_j\}$, where ρ_j corresponds to the vertex with the maximum index that belongs to S with $\rho_j \equiv y_1$ when $j = N + 1$. Since ρ_{j+1} doesn't belong to S, it follows that condition G_1 is satisfied for every subset V that contains only density vertices. Thus, in order to guarantee that condition G_1 is satisfied it is sufficient to show that for every subset $V \subseteq \{\rho_1, \ldots, \rho_N, r_1, \ldots, r_m\}$ (i.e., which contains vertices of the form r_i) there exists a vertex x that doesn't belong to V and, moreover, it is such that $V \cap \text{Post}\left(\{x\}\right)$ is a singleton. From Fig. 2 it is evident that the only cases the latter requirement may not

hold are the following. The subset V contains pairs of vertices of the form $\{r_i, \rho_{i-1}\}$ (namely an on-ramp vertex and a vertex that corresponds to the density of the segment immediately upstream of the segment with the on-ramp, respectively) and, potentially, every other vertex on the left of ρ_{i-1} (irrespectively of being a density or an on-ramp vertex), but it doesn't contain vertex ρ_i (or any other vertex, density or on-ramp, on the right of ρ_i). To see this, note that, otherwise, $V \cap \text{Post}(\{\rho_{i+1}\}) = \{\rho_i\}$ or, in the case where V contains only on-ramp vertices, $V \cap \text{Post}(\{\rho_i\}) = \{r_i\}$. Thus, one can conclude that condition G_1 is satisfied when a mainstream total flow fixed detector is placed at segment $i-1$, namely at the segment immediately upstream of the segment with the on-ramp, since then $V \cap \text{Post}(\{y_i\}) = \{\rho_{i-1}\}$. In other words, condition G_1 holds when an output vertex y_i exists as shown in Fig. 2.

The fact that the existence of the output vertex y_i is also necessary for the satisfaction of condition G_1 (and thus, necessary for strong structural observability [38]) follows from the previous discussion by taking $V = \{r_i, \rho_{i-1}\}$ and noting that the only vertex that has a successor in V (but, it doesn't belong to V) is ρ_i which, however, has two successors in V. Finally, the fact that the existence of the output vertex y_1 is a necessary condition for G_1 to hold, can be shown by taking $V = \{\rho_N\}$ and noting that there exists no vertex which doesn't belong to V with a successor in V.

b) Claim 2: The corresponding graph $\mathcal{G}\left(\mathcal{A}^{\mathrm{T}}, \mathcal{C}^{\mathrm{T}}\right)$ for Model II is shown in Fig. 3. It is evident from Fig. 3 that strong structural observability is preserved under the same mainstream, fixed total flow measurement requirements as in the single-lane case (i.e., as in Claim 1). Note that a red edge may not exist, if the corresponding lateral flow of connected vehicles is zero, without affecting the strong structural observability of the system.

The fact that the measurement configuration i) and ii) of Claim 2 is also necessary for strong structural observability can be shown as follows. Consider the case where, e.g., the output vertex y_1 doesn't exist. Then, in the case in which the red edge from χ_N to ϕ_N doesn't exist, condition G_1 obviously cannot hold for $V = \{\phi_N\}$. The necessity of the measurement configuration ii) follows analogously with Claim 1, by choosing the set $V = \{\phi_{i-1}, r_i\}$ and considering a case in which there is no red edge from χ_{i-1} to ϕ_{i-1}. The only vertex that has a successor in V (but, doesn't belong to V) is ϕ_i which, however, has two successors in V.

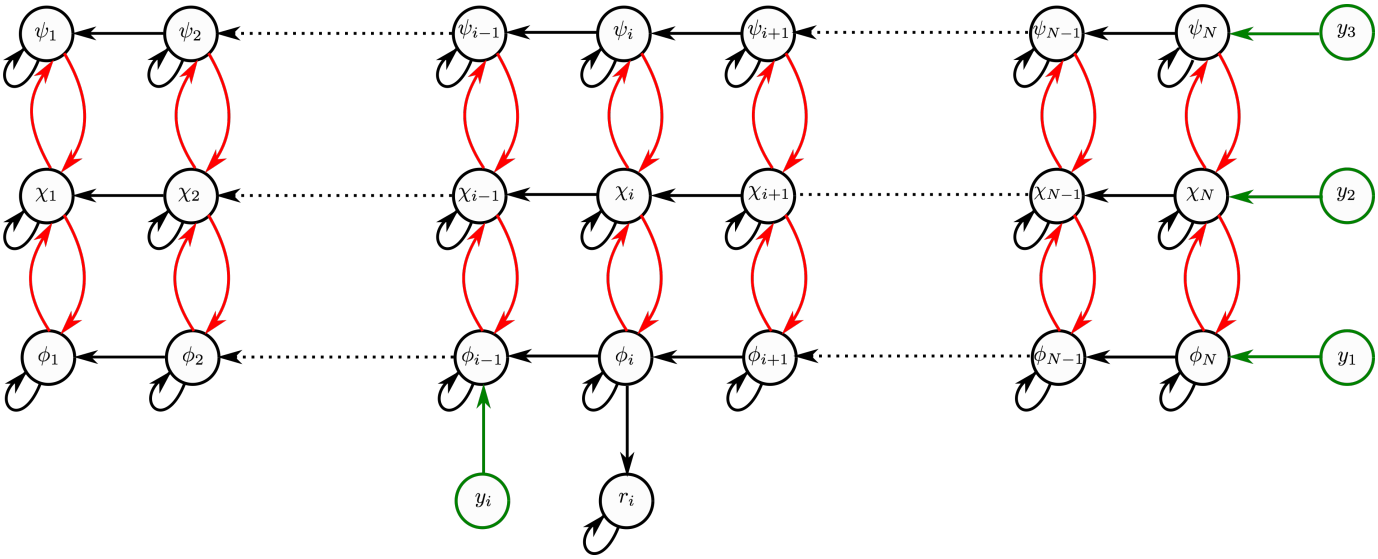

Fig. 3. The graph $\mathcal{G}\left(\mathcal{A}^{\mathrm{T}}, \mathcal{C}^{\mathrm{T}}\right)$ for patterns $\mathcal{A}$ and $\mathcal{C}$ that include matrices A and C, respectively, of system (10), (11), for the case of a three-lane highway stretch with $\bar{p}_{i,j} = p_{i,j} = 0$, for all i and j, when the lateral flows of connected vehicles may be nonzero (Model II).

c) Claim 3: We next turn our attention to Model III, i.e., to the most general case of highway stretches modeled by system (10), (11), where the percentage values of diagonal on-ramp or lateral flows may be nonzero. The corresponding graph $\mathcal{G}\left(\mathcal{A}^{\mathrm{T}}, \mathcal{C}^{\mathrm{T}}\right)$ is shown in Fig. 4. Unfortunately, condition G_0

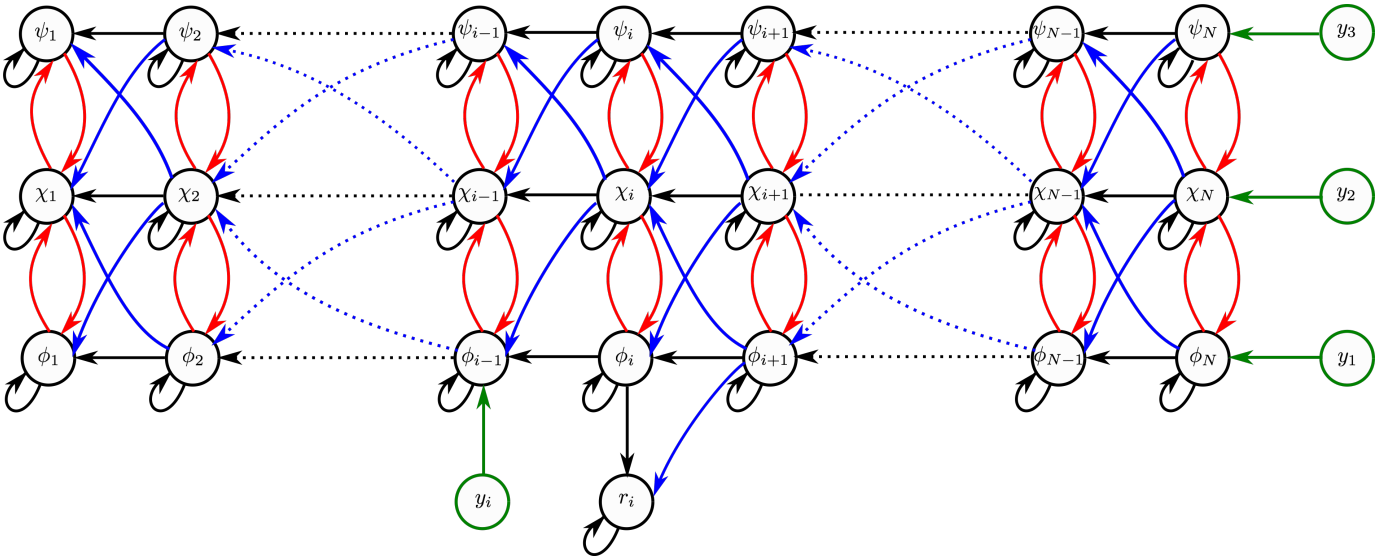

Fig. 4. The graph $\mathcal{G}\left(\mathcal{A}^{\mathrm{T}}, \mathcal{C}^{\mathrm{T}}\right)$ for patterns $\mathcal{A}$ and $\mathcal{C}$ that include matrices A and C, respectively, of system (10), (11), for the case of a three-lane highway stretch where the percentage values of diagonal on-ramp or lateral flows may be nonzero (Model III).

cannot be satisfied for this general highway stretch with the measurement configuration shown in Fig. 4. This can be seen, for example, by choosing the set $\{\phi_1, \chi_1, \psi_1\}$ since there exists no vertex x such that

the set $\{\phi_1, \chi_1, \psi_1\} \cap \text{Post}(\{x\})$ contains only one element[7].

d) Claim 4: For Model IV, condition G_1 cannot be satisfied for subsets V of the form $\{\phi_i, r_i\}$. This can be seen from Fig. 4, for the special case of one lane, as follows. The only vertex that doesn't belong to V and has a successor in V is ϕ_{i+1}, which, however, has two successors in V.

F. (Weak) Structural Observability of Lane-Based Highway Traffic

We establish the following claims for each of the models I–VI:

5. Model V is (weakly) structurally observable if and only if: i) total flow fixed detectors are placed at the main exit of the considered highway stretch; and ii) for each pair of on-ramps, an additional fixed flow sensor is placed anywhere between two consecutive on-ramps.
6. Model I is (weakly) structurally observable under the measurement configuration i) and ii) of Claim 5.
7. Model I is (weakly) structurally observable if and only if total flow fixed detectors are placed at the main exit of the considered highway stretch.
8. Model VI is (weakly) structurally observable if and only if: i) for each pair of on-ramps, an additional fixed flow sensor is placed anywhere between two consecutive on-ramps; and either iia) total flow fixed detectors are placed at the main exit of every lane of the considered highway stretch, when some lateral flows of connected vehicles may be zero; or iib) total flow fixed detectors are placed at the main exit of at least one of the lanes of the considered highway stretch, when all lateral flows of connected vehicles are always nonzero.
9. Model III is (weakly) structurally observable under the measurement configurations i) and iia) or i) and iib) of Claim 8.
10. Model III is (weakly) structurally observable if and only if: either ia) total flow fixed detectors are placed at the main exit of every lane of the considered highway stretch, when some lateral flows of connected vehicles may be zero; or ib) total flow fixed detectors are placed at the main exit of at least one of the lanes of the considered highway stretch, when all lateral flows of connected vehicles are always nonzero.

[7]Note that for not making the corresponding graph shown in Fig. 4 more complex than needed, we consider the case where the total flows measured at the segments with mainstream fixed detectors are modeled by (4), with the percentage values of diagonal flows equal to zero. The conclusion drawn is not changed when some of the corresponding percentage values are nonzero.

Note that Claims 9, 10 and Claims 6, 7 trivially extend to Model II and Model IV, respectively, and thus, they are not presented here. One can see this by observing that the proofs of Claims 6, 7, 9, and 10 are not affected by the existence or not of blue edges, i.e., of edges due to non-zero percentages.

a) Claim 5: We start by constructing the graph $\mathcal{G}\left(\bar{\mathcal{A}}^{\mathrm{T}}, \mathcal{C}^{\mathrm{T}}\right)$, shown in Fig. 5, where $\bar{\mathcal{A}} = \frac{1}{T}\left(\mathcal{A} - \mathcal{I}\right)$.

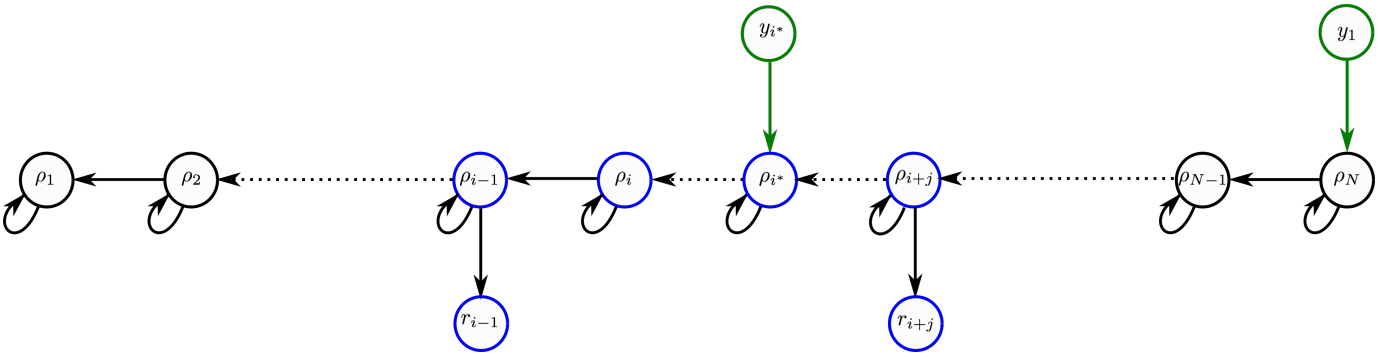

Fig. 5. The graph $\mathcal{G}\left(\bar{\mathcal{A}}^{\mathrm{T}}, \mathcal{C}^{\mathrm{T}}\right)$ for patterns $\bar{\mathcal{A}} = \frac{1}{T}\left(\mathcal{A} - \mathcal{I}\right)$ and $\mathcal{C}$ that include matrices A and C, respectively, of system (10), (11), for the case of a simple one-lane highway stretch with N segments (Model V).

Utilizing the results, e.g., from [25], [27], the one-lane highway stretch is (weakly) structurally observable if the graph $\mathcal{G}\left(\bar{\mathcal{A}}^{\mathrm{T}}, \mathcal{C}^{\mathrm{T}}\right)$, shown in Fig. 5, contains no non-accessible vertex and no dilation. A necessary and sufficient condition for the graph to contain no non-accessible node is that a fixed flow sensor is placed at the exit of the considered highway stretch, or, in other words, that an output vertex y_1 is placed as shown in Fig. 5. Moreover, from Fig. 5 one can observe that every density vertex contains a self-edge, and hence, every density vertex has at least two predecessors. Therefore, the only possibility for a dilation to exist is when one considers subsets of vertices like the ones indicated in blue circle in Fig. 5 (i.e., when one considers subsets of vertices that include two consecutive on-ramp vertices together with the density vertices at and between the cells with the on-ramps). Thus, no dilation exists if and only if an additional fixed flow sensor is placed anywhere between two consecutive on-ramps, as it is indicated in Fig. 5 with the output vertex y_{i^*}. With the same reasoning, it is easy to conclude that, in case there is only one on-ramp, one sensor only, namely a sensor at the exit of the considered highway stretch, is sufficient and necessary for (weak) structural observability.

b) Claim 6: The total flow measurement configurations in Claim 5 above are sufficient for the (weak) structural observability of the original system of pattern $\mathcal{A}$ since the graph $\mathcal{G}\left(\mathcal{A}^{\mathrm{T}}, \mathcal{C}^{\mathrm{T}}\right)$ is similar to the graph $\mathcal{G}\left(\bar{\mathcal{A}}^{\mathrm{T}}, \mathcal{C}^{\mathrm{T}}\right)$, with the only addition that there are self-edges at all on-ramp vertices. In fact, it is

not difficult to see in Fig. 5 that with the addition of self-edges at the on-ramp vertices, there is still no non-accessible vertex, and, in addition, there exists no dilation since every state vertex has a self-edge.

c) Claim 7: For graph $\mathcal{G}\left(\mathcal{A}^{\mathrm{T}}, \mathcal{C}^{\mathrm{T}}\right)$ the existence of only one output vertex, namely of y_1 (that corresponds to a fixed flow sensor at the exit of the considered highway stretch), is sufficient for (weak) structural observability. This can be seen by observing from Fig. 2 that all state vertices have a self-edge, thus no dilation occurs, and, all state vertices are accessible from the output vertex y_1. Necessity is not difficult to establish by observing that when the output vertex y_1 is not located at the position shown in Fig. 2, the vertex ρ_N cannot be accessible.

The motivation for studying Models V and VI is explained in the next remark.

Remark 1: For physical systems, (weak) structural observability is usually sufficient for observability since "a possible loss of observability of a (weakly) structurally observable system can occur only in pathological cases when there are accidental constraints of the system parameters", as it is stated in [26]. Yet, the random walk dynamics that we introduce, which correspond to diagonal elements of matrix A that are equal to each other (in fact, they are all exactly equal to one), impose some rather non-physical interconnections in model (10). In principle, such fictitious dependencies/symmetries among specific elements of matrix A may cause a (weak) structural observability test to eventually underestimate the number of sensors needed for observability, see, e.g., [27][8]. The following example illustrates this fact.

Example 1: Consider the case of an one-lane highway stretch with two segments and two on-ramps, where free-flow conditions prevail (assume zero percentages of on-ramp diagonal flows). The A and C matrices of system (10), (11) reduce in this case to

$$A = \begin{bmatrix} 1-\frac{T}{\Delta}v_f & 0 & \frac{T}{\Delta} & 0 \\ \frac{T}{\Delta}v_f & 1-\frac{T}{\Delta}v_f & 0 & \frac{T}{\Delta} \\ 0 & 0 & g_1 & 0 \\ 0 & 0 & 0 & g_2 \end{bmatrix} \tag{18}$$

$$C = \begin{bmatrix} 0 & v_f & 0 & 0 \end{bmatrix}, \tag{19}$$

respectively, where the elements of the A matrix that correspond to the random walk dynamics have been

[8]There may be additional symmetries due to, e.g., in the case of one-lane highway, terms of the form $1-\frac{T}{\Delta}v_{i,j}$ and $\frac{T}{\Delta}v_{i,j}$ that appear in the main diagonal and the diagonal immediately below of matrix A, respectively. However, such dependencies don't seem to cause an underestimation of the measurement requirements needed for observability since such symmetries/dependencies are inherent to the actual physical system.

replaced by some arbitrary values g_1 and g_2 (instead of one). It can be shown that the determinant of the observability matrix (see paragraph *f)* in the Appendix) $O = \begin{bmatrix} C \\ CA \\ CA^2 \\ CA^3 \end{bmatrix}$ is given by

$$\det(O) = \frac{T^4 v_f^6}{\Delta^5} (g_1 - g_2) (\Delta g_2 - \Delta + T v_f) . \tag{20}$$

From (20) it is clear that, irrespectively of the values for v_f, T, and Δ, the system is not observable (i.e., the determinant of the observability matrix is zero), when the on-ramp flow dynamics are identical to each other (which is the case when both on-ramp flow dynamics are modeled by random walk equations), i.e., when $g_1 = g_2$[9], although according to Claim 7 Model I is (weakly) structurally observable.

Models V and VI could be viewed as approximations of the continuous-time version of Models I and III, respectively (see Section III-D for details). As such, the dynamics of the deterministic part of a random walk equation (modeling the on-ramp flows) are zero. Replacing in the random walk equations the corresponding ones with fixed zeros, breaks potential fictitious symmetries in the structure of the system, which may appear. Thus, compared to the discrete-time case, it is more likely that the resulting conditions for (weak) structural observability are more physically oriented as well as sufficient. Indeed, when Models V and VI are (weakly) structurally observable, then Models I and III are so, since the addition of edges never weakens the (weak) structural observability of a system (see, e.g., [25], [27]).

d) Claim 8: The graph for Model VI is identical to the graph of Fig. 4 with the only difference that on-ramp vertices have no self-edges. Observe next that the graph of Model VI is derived by the graph of Model V, shown in Fig. 5, by adding extra edges that correspond to diagonal flow percentages or lateral flows of connected vehicles, as well as extra vertices that correspond to densities of additional lanes. One can show that these additional edges and vertices don't affect the (weak) structural observability of the system under the measurement configuration of Claim 5 as follows. Since every additional state vertex has a self-edge, still no dilation occurs. Furthermore, all state vertices are accessible by an output vertex when there are measurements in all lanes at the exit of the considered highway stretch, no matter if lateral flows of connected vehicles are zero or not. Finally, in the case where there is a measurement at at least one lane at the exit of the stretch, it can be seen that all state vertices are still accessible by an output

[9]From (20) one can observe that the system is not observable also in the case where $g_2 = \frac{\Delta - T v_f}{\Delta}$. However, the latter condition is just an accidental condition without any meaningful physical interpretation.

vertex as long as the lateral flows of connected vehicles are always nonzero (i.e., the red edges always exist).

The fact that the measurement configuration i) of Claim 8 is also a necessary condition for (weak) structural observability can be shown as follows. Consider the set of blue vertices in Fig. 5 and assume that there is no incoming edge to that particular set, which could potentially exist due to nonzero percentages of diagonal flows or due to nonzero lateral flows to the adjacent lane. Then this set contains a dilation when the output vertex y_i^* doesn't exist, and hence, the system is not (weakly) structurally observable. Moreover, the measurement configuration iia) is a necessary condition for (weak) structural observability, which can be seen from Fig. 4 as follows. Consider, for example, the case in which there is no output vertex y_3, and, in addition, the red edge from χ_N to ψ_N doesn't exist. Then the vertex ψ_N is non-accessible, and thus, the system is not (weakly) structurally observable. Finally, it is trivial to show that the measurement configuration iib) is a necessary condition for (weak) structural observability since when condition iib) doesn't hold there is no output vertex at the exit of any lane. Hence, all vertices of every segment on the right of some segment with an output vertex y_i are non-accessible.

e) Claims 9 and 10: The proofs of Claims 9 and 10 follow easily from Claim 8 employing similar arguments to the proof of Claims 6 and 7, respectively.

In a nutshell, the general model (10), (11) was shown to be strongly structurally observable when all percentage values for diagonal flows are set to zero if flow detectors are placed at the main exit and entry in each lane of the considered highway stretch as well as at every segment immediately upstream of a segment with an on-ramp. Yet, when some percentages of diagonal flows are not zero the system may not be strongly structurally observable under this detector configuration. As far as (weak) structural observability is concerned, it was shown that the general system (10), (11) is (weakly) structurally observable if flow detectors are placed at the main exit and entry of every lane of the considered highway stretch as well as if, for each pair of on-ramps, an additional flow sensor is placed anywhere between two consecutive on-ramps (no extra sensor is needed when there is only one on-ramp).

Note that the (weak) structural observability results of this section concern the time-invariant version of matrices A and C with the structure $\mathcal{A}$ and $\mathcal{C}$, respectively. However, adapting the results from [33], [34] (see also, [26], [32]) to the case of the observability matrix one can conclude that the original time-

varying system (10), (11) is (weakly) structurally observable as well. This can be shown by noting that the observability matrix that corresponds to the time-varying version of matrices A and C, having the structure $\mathcal{A}$ and $\mathcal{C}$ for all times, has a generic rank $MN+m$, on any interval of the form $[k_0, k_0+MN+m]$, for all $k_0 \geq 0$. The latter conclusion follows by combining the results in [33], [34] with the (weak) structural observability results of this section, and noting that the elements of matrices A and C are well-defined, explicit functions of speeds, lateral flows, and densities of connected vehicles (which are all assumed to be uniformly bounded from above and, in addition, speeds and densities are assumed to be positive and uniformly bounded from below, see Sections II-C and III-E).

G. Stability of the Estimation Scheme

We state first the following claim.

11. The Kalman filter (12)–(14) is exponentially stable if system (10), (11) is strongly structurally observable.

We now prove Claim 11.

a) Claim 11: We employ the results from [30] provided for the reader's benefit in paragraph *i)* in the Appendix. The matrices A and C are continuous functions of speeds, lateral flows, and densities of connected vehicles since densities of connected vehicles are assumed to be positive. Given that speeds, lateral flows, and densities of connected vehicles are all assumed to be uniformly bounded from above, and, additionally, densities are assumed to be uniformly bounded from below (see also Sections II-C and III-E), one can conclude that the matrices A and C are bounded. Moreover, the matrices Q, R, and R^{-1} can be made bounded above since Q and R can be freely chosen, and thus, they may be chosen as $Q=\sigma_1 I$ and $R=\sigma_2 I$, where $\sigma_1, \sigma_2 > 0$ and I denotes the identity matrix of appropriate dimension. The freedom to choose $Q=\sigma_1 I$ automatically implies that the pair (A, D) is uniformly completely reachable[10] (UCR) with $D=\sqrt{\sigma_1} I$, since the dimension of D equals the dimension of the A matrix. It remains to show that the pair (A, C) is uniformly completely observable[11] (UCO) provided that system (10), (11) is strongly structurally observable.

Combining the results of Section III-E with Corollary IV.2 from [38] as well as with Theorem IV.2 and

[10] See paragraph *h)* in the Appendix for the definition of UCR.
[11] See paragraph *g)* in the Appendix for the definition of UCO.

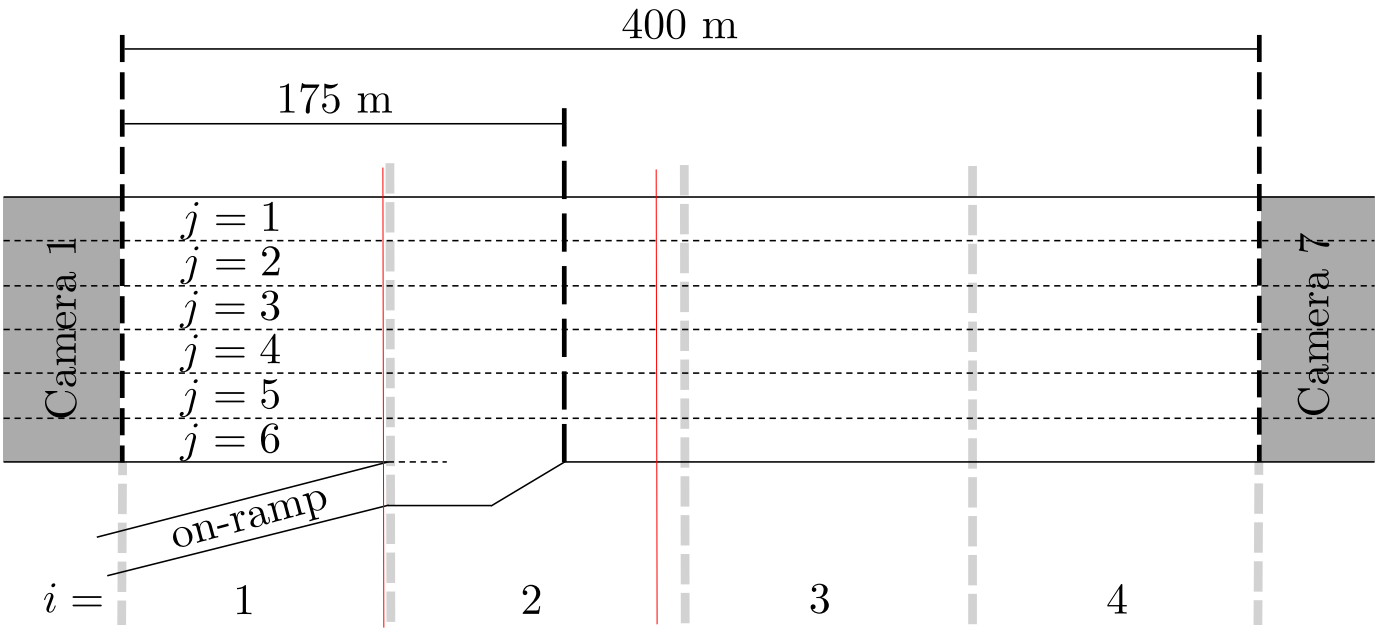

Fig. 6. Graphical representation of the considered stretch of highway I-80 in Emeryville, California, employed in the evaluation of the estimation scheme with NGSIM data.

Corollary IV.3 from [16], one can conclude that every system (10), (11) with structure $(\mathcal{A}, \mathcal{C})$ is observable on any interval of the form $[k_0, k_0 + MN + m]$, for all $k_0 \geq 0$, when system (10), (11), of structure $(\mathcal{A}, \mathcal{C})$ is strongly structurally observable. Thus, the observability Gramian (see paragraph *d)* in the Appendix) $G(k_0, k_0 + MN + m)$ (see, e.g., [30]) is positive definite for all $k_0 \geq 0$. The latter implies that, for each k_0, the observability Gramian is upper and lower bounded by its maximum and minimum eigenvalues (times the identity matrix), respectively, which are both positive. Therefore, the system is UCO if for each k_0 the maximum and minimum eigenvalues of the observability Gramian are positive as well as uniformly bounded from above and below from constants independent on k_0. This holds true because the elements of the matrices A and C are continuous functions of speeds, lateral flows, and densities of connected vehicles, which are all assumed to be uniformly bounded from above, and, additionally, speeds and densities are assumed to be positive and uniformly bounded from below (see Sections II-C and III-E).

IV. Performance Evaluation Using NGSIM Data

A. Highway Stretch and Data Computation Descriptions

a) Highway Stretch Description: The highway stretch considered in the evaluation of the developed estimation scheme is shown in Fig. 6. It is a 400-meter long stretch in the northbound direction of I-80 in Emeryville, California. The highway stretch is composed of six lanes, where the left-most lane is a

so-called high occupancy-vehicle (HOV) lane, which is characterized by the fact that access is restricted to a limited set of vehicles (only vehicles with a driver and one or more passengers are allowed), and thus, the traffic flow states in the HOV lane are structurally different compared to the rest of the lanes. Moreover, an on-ramp is entering the mainstream, the merging nose being located 175 meters away from the beginning of the stretch. For the purpose of estimation, the stretch is divided into four 100-meter long segments.

b) Data Computation Description: We employ a processed version of NGSIM vehicle trajectory data, recorded from 4:00 PM to 4:15 PM on April 13, 2005, from [28], [29]. All the required measurements utilized by the estimation scheme as well as those used for computing the ground truth traffic state are produced from the available trajectory data as follows.

Data employed by the estimator:

- Vehicles entering the highway stretch are randomly marked as connected, according to the considered penetration rate, based on a uniform distribution. The measured average cell speeds, namely, v^{c}, employed by the estimator are computed as the arithmetic average of the speeds of connected vehicles that are present within a cell at a time instant kT, where $T = 5$ seconds is the execution period of the estimation scheme. If there is no connected vehicle at a time instant kT then the measured average speed of the specific cell is set equal to the previous one[12].
- The measured lateral flows of connected vehicles, namely, L^{c}, are produced by counting the number of connected vehicles that moved from one lane to another during a time interval $(kT, (k+1)T]$. Moreover, the cell densities of connected vehicles, namely, ρ^{c}, are computed by counting the number of connected vehicles that are present within a cell at time instant kT divided by the cell length. Because terms of the form $\frac{L^{\mathrm{c}}}{\rho^{\mathrm{c}}}$ may contain several spiky values, especially at low penetration rates, mainly due to the rare appearance of connected vehicles' at a time instant kT (and thus, also the rare appearance of lateral movements), we employ in the estimation scheme an exponentially smoothed version of the originally computed terms of the form $\frac{L^{\mathrm{c}}}{\rho^{\mathrm{c}}}$. Specifically, we define for all $i = 1, \ldots, N$,

[12]Note that, in the case in which there is no connected vehicle at $k = 0$ in specific cells, the measured average cell speeds $v_{i,j}(0)$ of those cells are computed as the average of the cell speeds over all cells and over the whole simulation horizon. In an actual implementation this case is virtually irrelevant as the estimation scheme is operated continuously.

$j_1 = 1, \ldots, M$, and $j_2 = j_1 \pm 1$ the following smoothed version of a term of the form $\frac{L^{\mathrm{c}}}{\rho^{\mathrm{c}}}$

$$\bar{S}^{\mathrm{c}}_{i,j_1 \to j_2}(k+1) = (1-\alpha)\, \bar{S}^{\mathrm{c}}_{i,j_1 \to j_2}(k) + \alpha \frac{L^{\mathrm{c}}_{i,j_1 \to j_2}(k)}{\rho^{\mathrm{c}}_{i,j_1}(k)}, \tag{21}$$

where the factor α belongs to the interval $[0, 1]$ and the initial conditions $\bar{S}^{\mathrm{c}}_{i,j_1 \to j_2}(0)$ are viewed as tuning parameters and are yet to be chosen.

Note that the problem, at some time instants, of the possible division with zero in relation (21) is resolved by setting the term $\frac{L^{\mathrm{c}}_{i,j_1 \to j_2}}{\rho^{\mathrm{c}}_{i,j_1}}$, equal to zero. This is motivated by the fact that when the reported density of connected vehicles is zero, i.e., when there is no connected vehicle present in a cell, then it is reasonable to assume that the corresponding lateral flow of connected vehicles is also zero, thus no new information is provided as input to the dynamic equation (21) of the smoothed variable. One could resolve the problem of the possible division with zero in relation (21) by employing other simple ways, such as, for example, by replacing the zero values for the density of connected vehicles by non-zero values that are computed utilizing a moving average, over a certain horizon, of previous (non-zero) density values.

- Total flow measurements at the entry and exit of the stretch, namely, y and u, respectively, are produced via two respective series of virtual spot detectors, one placed in all lanes at the entrance of the considered highway stretch and another placed in all lanes at the exit of the highway stretch, where the corresponding flow values are produced by counting the number of vehicles (irrespectively of being connected or not) that cross the virtual detector locations during the corresponding periods.
- Total speed measurements at the exit of the considered stretch, i.e., at each of the last cell of every lane, say, $v^{\mathrm{m}}_{4,j}$, $j = 1, \ldots, 6$, are computed as the arithmetic average at time instant kT of the speeds of all vehicles that are present within each cell.

Note that since we assume anyway the availability of flow detectors at the exit of the stretch, it is reasonable to assume that speed measurements from detectors may be available as well. For this reason, we replace the corresponding speeds v^{c} in the output equation (11) by the speeds v^{m}. Alternatively, when occupancy detectors are available instead, the densities at the exit of the stretch may be directly extracted. In this case, all elements of the C matrix in (11) would simply be equal to one. In general, we expect small variations in the estimation performance among these cases, so we present only one of them. Finally, note

that since there is only one unmeasured on-ramp within the considered highway stretch only the total flow measurements at the entry and exit of the stretch are needed for observability, and thus, for the proper operation of the estimation scheme (see Section III).

Data for ground truth generation:

- The total cell densities are computed by counting the number of all vehicles that are present within a cell at a time instant kT divided by the segment length.
- The on-ramp flow is computed similarly to the lateral flows, i.e., by counting the number of vehicles leaving the on-ramp "lane" and entering the mainstream during time interval $(kT, (k+1)T]$.

B. Traffic Conditions Description

The reported traffic conditions reported in the HOV lane and the rest of the lanes can be shown in Figs. 7 and 8, respectively. Aggregated vehicle speeds $v_{i,j}$ are computed, for each cell, as the arithmetic average at time instant kT of the speeds of all vehicles that are present within each cell. As it can be seen from Fig. 7, free-flow conditions prevail in the HOV lane over the whole simulation period, whereas, as it is shown in Fig. 8, a massive congestion is present within the stretch in the rest of the lanes, where congestion waves are coming from downstream and crossing the entire stretch.

C. Performance Evaluation for Various Penetration Rates

a) Quantitative Performance Measure: The estimated densities and on-ramp flow used for evaluation are averages, over 30 seconds, of the produced estimates from the estimator. This allows us to deliver a more smooth version of the originally produced estimates, which are corrupted with noise due to the noisy/spiky values of the speed, lateral flow, and density of connected vehicles as well as of the total inflow and outflow at the considered stretch; but, most importantly, estimates at a pace of 30 seconds are at the lower end of the time resolution required for traffic control or other applications based on aggregated macroscopic traffic variables. The performance index is chosen as the average, over 10 replications, where in each replication a different set of vehicles is tagged as connected (due to the fact that, given a certain penetration rate, every vehicle that enters the considered highway stretch is randomly selected, from a uniform distribution, to be connected), of the Coefficient of Variation (CV) of the root mean square error

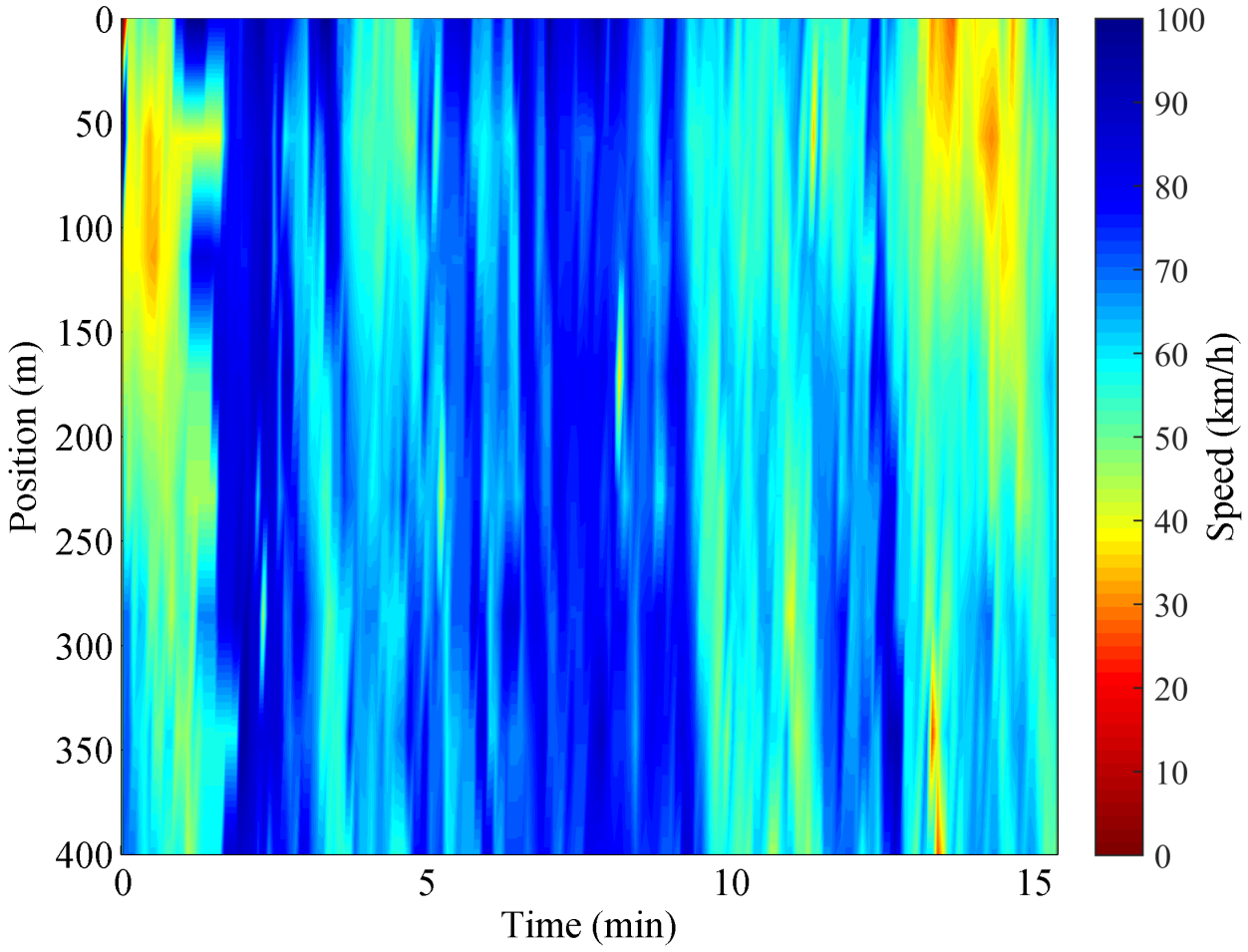

Fig. 7. The aggregated vehicle speeds of the HOV lane (lane $j = 1$) extracted from the NGSIM data. Free-flow conditions prevail in the HOV lave over the whole simulation period.

of the (30 second-averaged) estimated densities and on-ramp flow defined by

$$CV_\rho = \frac{\sqrt{\frac{1}{MNK}\sum_{i=1}^{N}\sum_{j=1}^{M}\sum_{k=1}^{K}\left(\rho_{i,j}(k)-\hat{\rho}_{i,j}(k)\right)^2}}{\frac{1}{MNK}\sum_{i=1}^{N}\sum_{j=1}^{M}\sum_{k=1}^{K}\rho_{i,j}(k)} \tag{22}$$

$$CV_r = \frac{\sqrt{\frac{1}{K}\sum_{k=1}^{K}\left(r(k)-\hat{r}(k)\right)^2}}{\frac{1}{K}\sum_{k=1}^{K}r(k)}, \tag{23}$$

respectively, where a quantity $\hat{w}$ indicates the estimate of w and $M = 6$, $N = 4$, $K = 23$.

b) Estimation Performance for a Baseline Case: In Fig. 9 we show the estimation results for the case of 20% penetration rate of connected vehicles (for one random replication, which is closest to the average performance). The parameters of the Kalman filter are defined as $Q = \text{diag}\left(\sigma_\rho I_{N\times M}, \sigma_r\right)$ (where σ_ρ corresponds to density estimation, whereas σ_r to the on-ramp flow estimation), $R = \sigma_R I_{M\times M}$, and $P(0) = I_{(N\,M+1)\times(N\,M+1)}$. For a fair comparison of the performance of the estimation scheme in

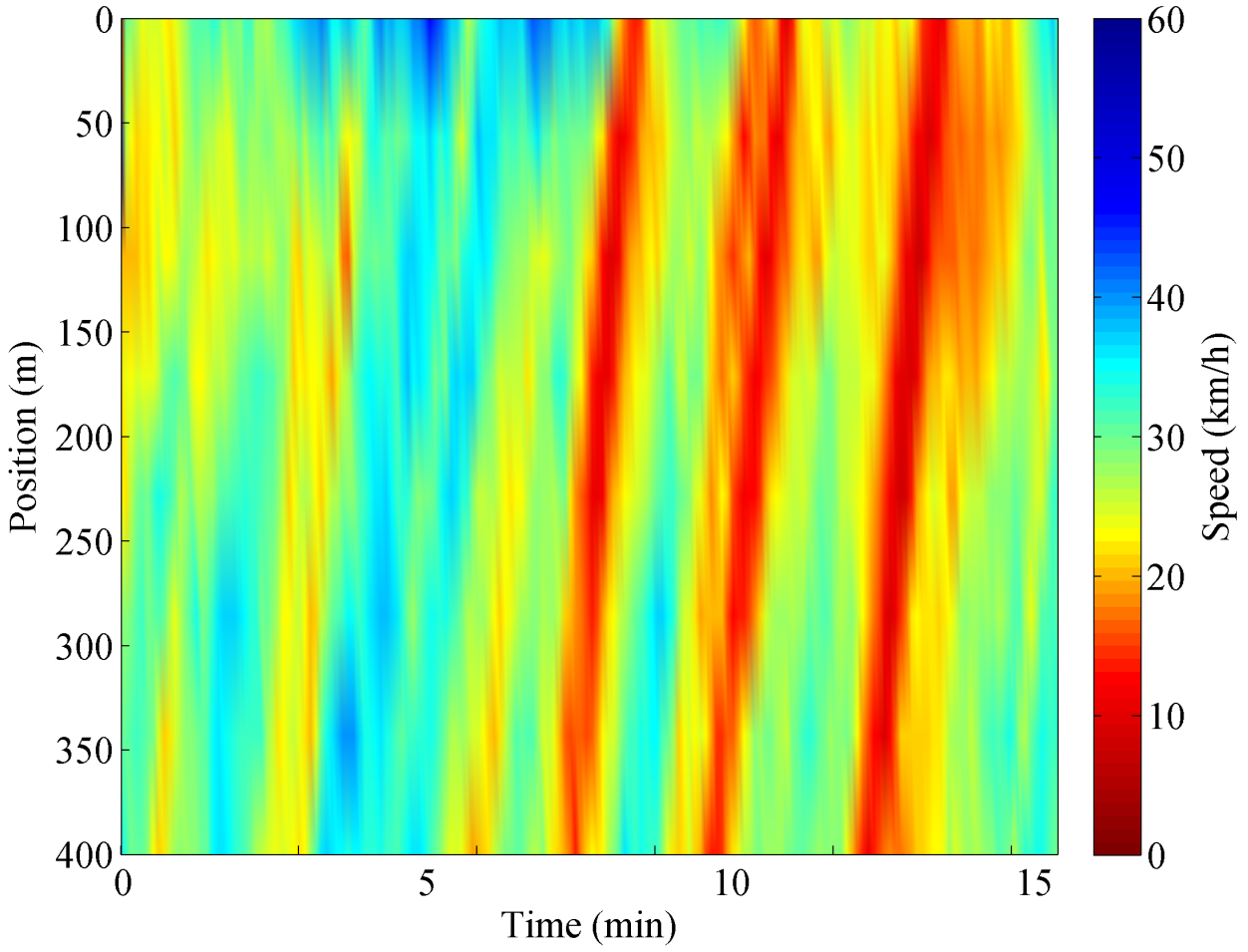

Fig. 8. The aggregated vehicle speeds of lanes $j = 2 \dots 6$ extracted from the NGSIM data. Congestion shock-waves are spilling back from downstream and cross the entire highway stretch.

quantitative terms, the filter is always initialized with the real density and on-ramp flow values, whereas the initial conditions for the filtered versions of the terms of the form $\frac{L_c}{\rho_c}$ are always set equal to zero. Moreover, only the percentage $\bar{p}$, modeling the diagonal lateral movement due to the on-ramps acceleration lane, where the effect of diagonal lateral movements is expected to be quite strong, has a non-zero value; all of the rest percentage values are set equal to zero. The estimation results are obtained with a percentage $\bar{p} = 0.3$, a smoothing factor $\alpha = 0.05$, and Kalman filter parameters $\sigma_\rho = 1$, $\sigma_r = 10$, $\sigma_R = 500$, resulting in $CV_\rho = 18\%$ and $CV_r = 41\%$.

From Fig. 9 it is evident that density estimation is quite accurate both during transient periods and at steady-state, considering also the high time and space resolution of the considered stretch and the available data. The on-ramp flow estimation is somewhat sluggish and it suffers from some delay, due to the distance

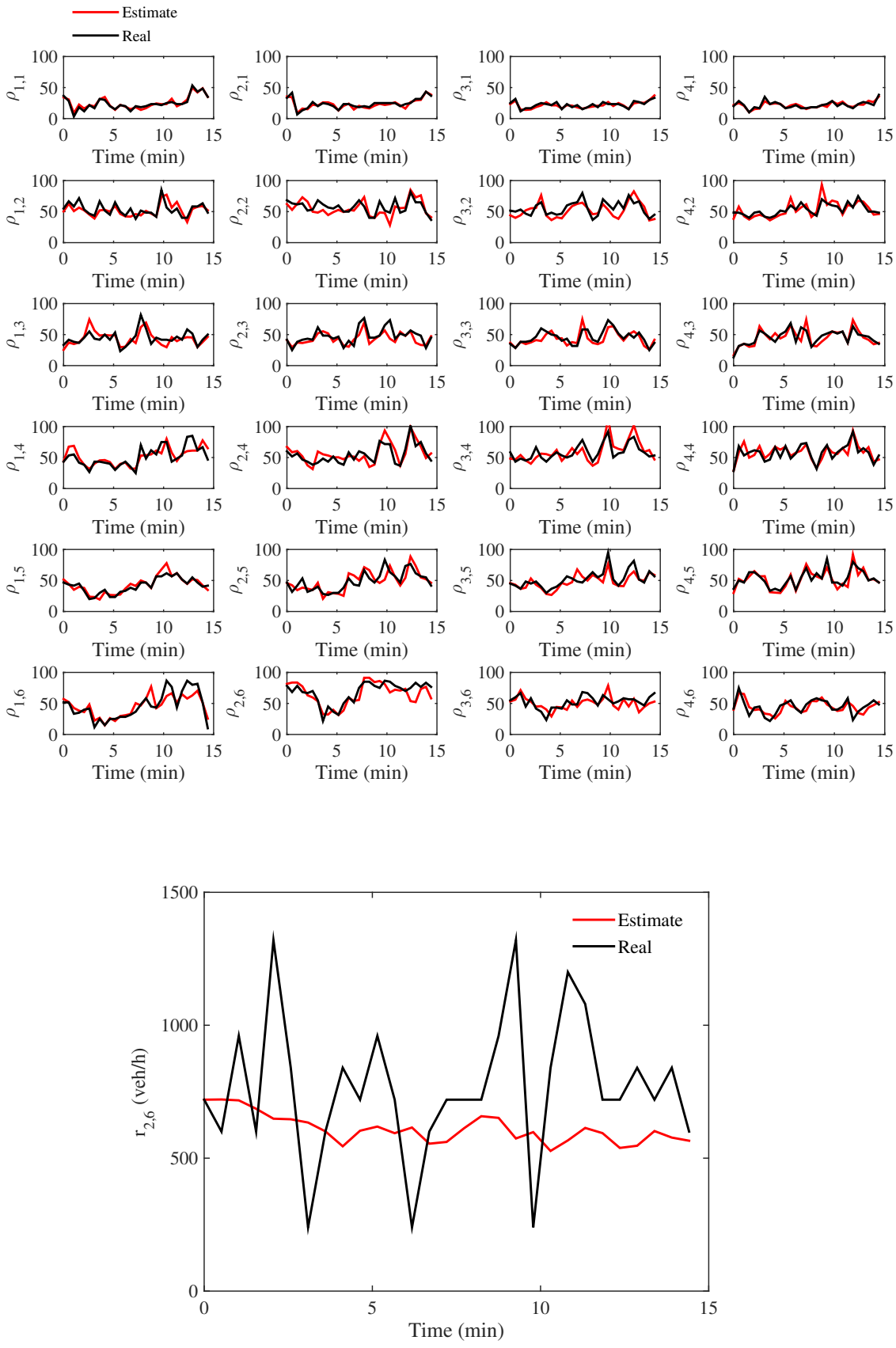

Fig. 9. Top: The estimated densities (red line) produced by the estimation scheme versus the real densities (black line) obtained from the NGSIM data. Bottom: The estimated on-ramp flow (red line) produced by the estimation scheme versus the real on-ramp flow (black line) obtained from the NGSIM data.

of the total flow detector at the exit of the considered stretch from the on-ramp location. One could make the response of the on-ramp flow estimation faster, by choosing a higher value for the element of the Q matrix that corresponds to the on-ramp flow estimation, yet, at the expense of making the estimation more "nervous" (or, in other words, more noisy). In fact, both the density and on-ramp estimation performance may be further improved by placing additional flow detectors. For example, whenever it is possible, an additional flow detector could be placed to measure directly the on-ramp flow (in order to not have to estimate it) or the flow at the mainstream cell immediately upstream of the cell where the on-ramp is located (to guarantee the strong structural observability of the system).

Note that the on-ramp flow estimation seems to feature a small bias (of the order of about $200\frac{\text{veh}}{\text{h}}$, which corresponds to a bias of $3\frac{\text{veh}}{\text{km}}$ in a mainstream cell), which can be explained as follows. In the model we employ for the lateral flow of connected vehicles, it is implied that the total lateral flow, within a time-interval $(kT, kT+T]$, is non-zero whenever there are connected vehicles at time instant kT. Although this appears to be a reasonable modeling implication and formally correct (considering the case of a 100% penetration rate of connected vehicles), it may be the case that, in practice, this doesn't happen. For example, there may be time instants at which the total lateral flow from the on-ramp lane to lane $j=5$ is non-zero, but this lateral flow is not taken into account by the model because vehicles may change lane without contributing to the density of lane $j=6$. Consequently, this "lost" flow, which originates from the on-ramp, causes an underestimation of the on-ramp flow. This problem may become more significant as the penetration rate reduces or when free-flow conditions prevail for a long time period since the density of connected vehicles may be zero quite often. However, this problem may be alleviated by reducing the estimator's implementation time step or by employing some other simple algorithm to replace the zero density values of connected vehicles, such as, for example, by replacing a zero density by previously reported non-zero density values or a moving average of those. Because such, somewhat heuristic approaches, may not be, *formally*, as accurate as the adopted approach, we don't employ them in the present work.

c) Comparison with a simple ad hoc estimation scheme: In order to further investigate and demonstrate the specific contribution of the developed estimation approach, we developed a less systematic, but still thoughtful and reasonable, ad hoc estimation scheme that computes density estimates by using

averaged information from connected vehicles. This simple scheme has similar data requirements as the proposed approach, albeit without the inherent quality properties and rigorous proofs that characterize the Kalman filter. Specifically, for the ad hoc estimator, we subdivide the highway into homogeneous cells (m, j), where m is the stretch index and j is the lane index; a stretch comprises all segments included between two ramps. We call these highway parts "homogeneous" because they include no ramp that would alter systematically the traffic conditions in the included segments. Thus, referring to Fig. 6, stretch $m = 1$ comprises only segment $i = 1$, while stretch $m = 2$ comprises segments $i = 2, 3, 4$. For each cell (m, j), we compute its corresponding average speed $\tilde{v}_{m,j}$ utilizing connected vehicle reports according to the method employed also for the case of the developed estimator; namely, $\tilde{v}_{m,j}$ is computed by averaging all speed reports from connected vehicles, which are located within each homogeneous cell (m, j). Using this speed and the available per-lane fixed-detector-measured total mainstream flow $\tilde{q}_{m,j}$ of the same stretch, we derive a density estimate for each cell (m, j), i.e., for all its segments (i, j), according to $\tilde{\rho}_{m,j} = \min\left(\frac{\tilde{q}_{m,j}}{\tilde{v}_{m,j}}, \rho^{\max}\right)$, where $\rho^{\max}$ is a reasonable upper-bound for density estimates, which is necessary since this estimation scheme may provide unrealistically high density values in case of low average speeds. In our experiment, we employ as upper-bound $\rho^{\max} = 180 \frac{\text{veh}}{\text{km} \times \text{lane}}$. Note that, in this experiment, we employ $\tilde{q}_{1,j} = q_{1,j}$ and $\tilde{q}_{2,j} = q_{4,j}$, which is a slightly different configuration than the one used in our estimation scheme.

Fig. 10 compares the density estimation performances obtained by using the ad hoc estimator and the developed estimation scheme. It is evident that the proposed approach produces consistently better estimation performance results for all tested penetration rates. Moreover, it is not clear how unmeasured on-ramp or off-ramp flows may be estimated employing the ad hoc scheme, while in our approach, this feature is included explicitly.

In summary, the ad hoc estimator is indeed less accurate, less general, and less flexible than the proposed systematic Kalman filter-based estimation scheme. Finally, we also would like to highlight that, despite our method may look more complex in formulation and derivation, it is not highly computationally demanding, since its execution requires only to calculate arithmetic averages and few matrix multiplications, which makes it feasible for real-time applications.

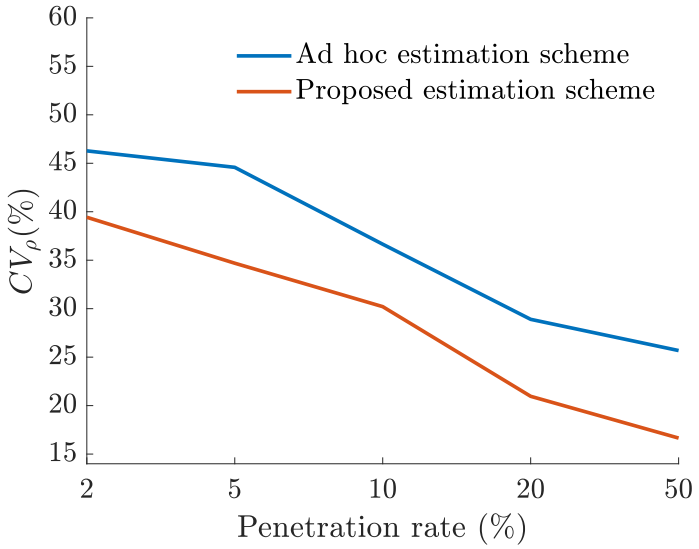

Fig. 10. Performance comparison of density estimation between the developed estimation scheme (red line) and the ad hoc estimation scheme (blue line) for various penetration rates of connected vehicles.

D. Sensitivity of the Estimation Performance to Variations of Parameters

a) Sensitivity of the Estimation Performance to Variations of the Parameters of the Kalman filter: We evaluate the performance index (22) obtained for a range of values for the parameters of the Kalman filter, namely σ_ρ, σ_r, σ_R, for various penetration rates. From Fig. 11, it is evident that the estimation scheme is quite insensitive to the choice of these parameters. This is in agreement with our previous findings in [5], [12], [40], where we show that, for the cross-lane estimation approach, density estimation is not sensitive to variations of the parameters Q and R.

b) Sensitivity of the Estimation Performance to Variations of the Percentage of On-Ramp Diagonal Flow: We show in Fig. 12 the performance indices (22), (23) obtained for various percentages of diagonal on-ramp flow and various penetration rates, whereas in Fig. 13 we show the performance index that corresponds only at the cell where the on-ramp is located. In Figs. 14 and 15 we show the same results for the case where the speed measurements employed by the estimator are a moving average, over a horizon of 30 seconds, of the speed measurements. In all experiments we use $\alpha = 0.05$, which was found to be a good value (see the discussion in paragraph *c)* below).

From Fig. 12 one can observe that the overall estimation performance is quite insensitive to changes of the parameter $\bar{p}$. Regarding density estimation, the optimal value for penetration rates higher than 20% is about $\bar{p} = 0.2$, whereas for lower penetration rates the optimal value increases with an average optimal

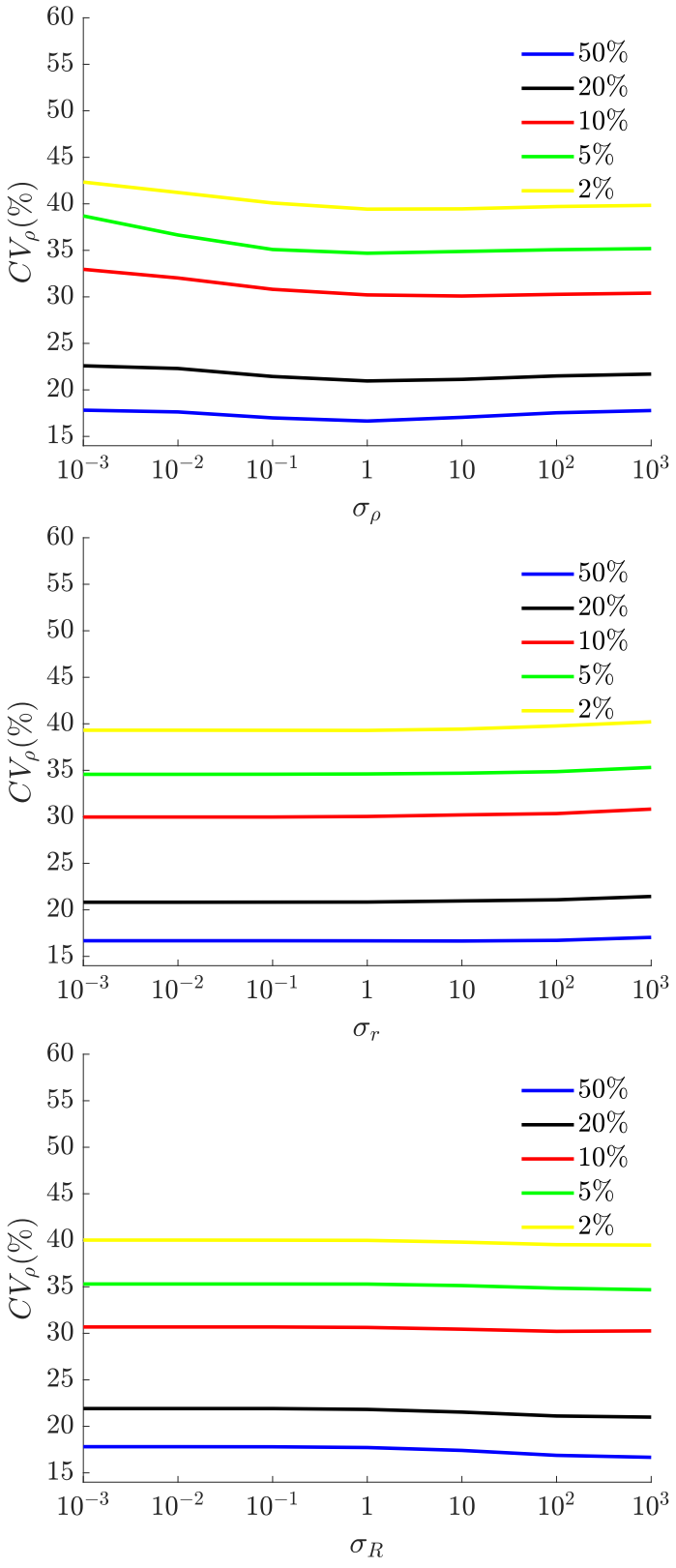

Fig. 11. Performance comparison of the density estimation for different values of the parameters σ_ρ (top), σ_r (middle), and σ_R (bottom), for various penetration rates of connected vehicles. Each parameter is evaluated independently, namely, maintaining the other two parameters constant and equal to the values used for the baseline case.

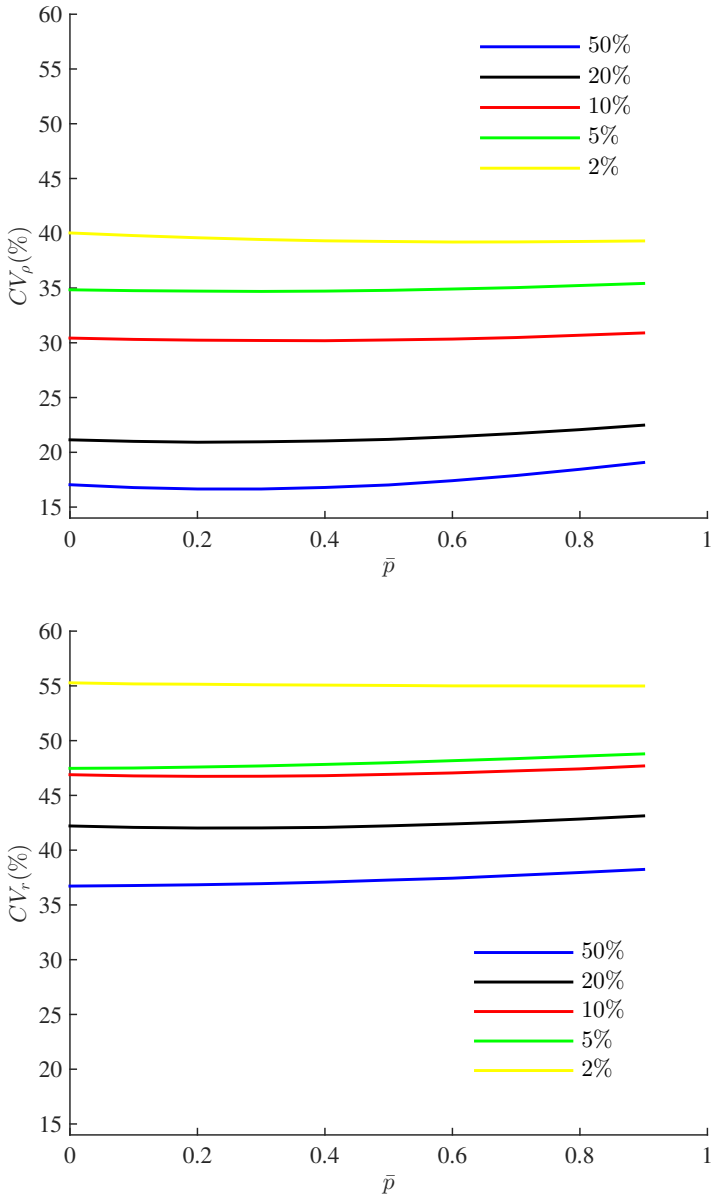

Fig. 12. Top: Performance index (22) versus percentage of on-ramp diagonal flow for various penetration rates of connected vehicles. Bottom: Performance index (23) versus percentage of on-ramp diagonal flow for various penetration rates of connected vehicles.

value for all penetration rates of about $\bar{p} = 0.36$. From Fig. 13 one can observe that the density estimation at the particular cell where the on-ramp is located is more sensitive to changes of the percentage $\bar{p}$. In fact, for almost all penetration rates the optimal value obtained is about $\bar{p} = 0.2$, whereas for the lowest penetration rate, namely, for 2%, the optimal value increases. This specific value may be attributed to the fact that, for the given highway stretch, the accelaration lane of the on-ramp is about 175 meters, and thus, its nose is close to the end of the cell, specifically at around two tenths before the end of the cell. Figs. 12 and 13 confirm, especially for low penetration rates, the need of imposing a non-zero percentage

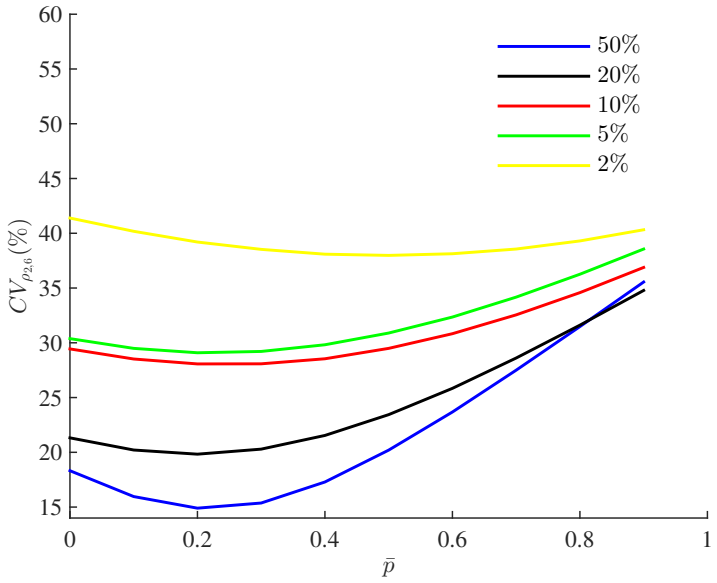

Fig. 13. Performance index (22) that corresponds to the cell in which the on-ramp is located versus percentage of diagonal on-ramp flow, for various penetration rates of connected vehicles.

$\bar{p}$. Similar comments may be made from Figs. 14 and 15, where it is evident that the main difference when employing a moving average for speed measurements is the improvement of the performance index at low penetration rates.

c) Sensitivity of the Estimation Performance to Variations of the Smoothing Factor: We show in Fig. 16 the performance indices (22), (23) obtained for $\bar{p} = 0.3$ and for various values of the smoothing factor α in (21) as well as various penetration rates, whereas in Fig. 17 we show the performance index (22) that corresponds to the estimation of the cell where the on-ramp is located. From Fig. 16 it is evident that the density estimation performance is quite insensitive to the variations of the smoothing factor, whereas the on-ramp flow estimation performance is more sensitive. In particular, one can observe from the bottom plot in Fig. 16 that the value of the smoothing factor at which the minimum of the performance index (23) is obtained almost decreases with the penetration rate, with an average value of about 0.055. This is consistent with the expectation that at lower penetration rates a stronger smoothing effect is needed.

Moreover, as it is evident from the top plot of Fig. 16, for the specific dataset used in our investigations, the incorporation of lateral flows in the estimation scheme does not play a major role in estimating the overall per-lane density. However, incorporating lateral flows in the estimation is beneficial for the estimation performance of the on-ramp flow and the density at the mainstream cell in which the on-ramp

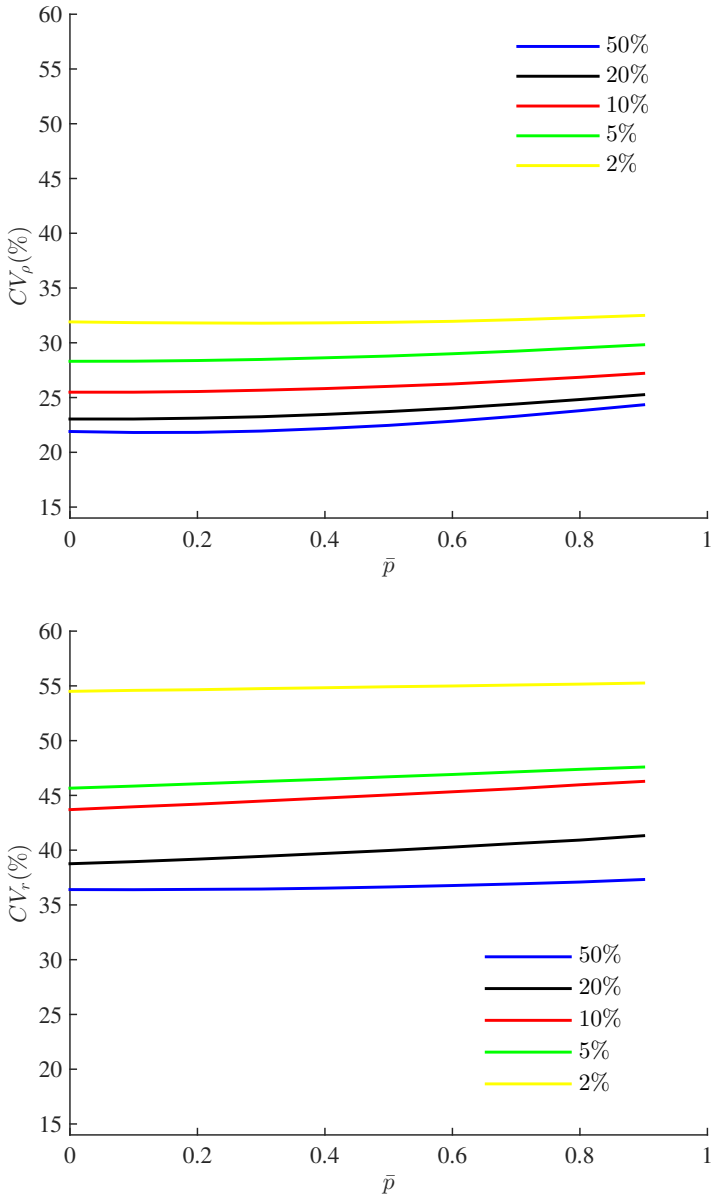

Fig. 14. Top: Performance index (22) versus percentage of diagonal on-ramp flow for various penetration rates of connected vehicles, where a moving average, over a horizon of 30 seconds, of the speed measurements is employed. Bottom: Performance index (23) versus percentage of diagonal on-ramp flow for various penetration rates of connected vehicles, where a moving average, over a horizon of 30 seconds, of the speed measurements is employed.

is located, as it is evident from the bottom plot in Fig. 16 and in Fig. 17, since for almost all penetration rates the performance index deteriorates for $\alpha = 0$ in comparison to the minimum value of the index that can be achieved choosing a non-zero value for α. These conclusions are reasonable since it is expected that, taking into account in the estimation the effect of lateral flows (via the lateral flow model), would be more beneficial at locations where strong lateral movements are observed (e.g., at an on-ramp location).

Furthermore, from Fig. 17 one can observe that for large values of the smoothing factor the performance

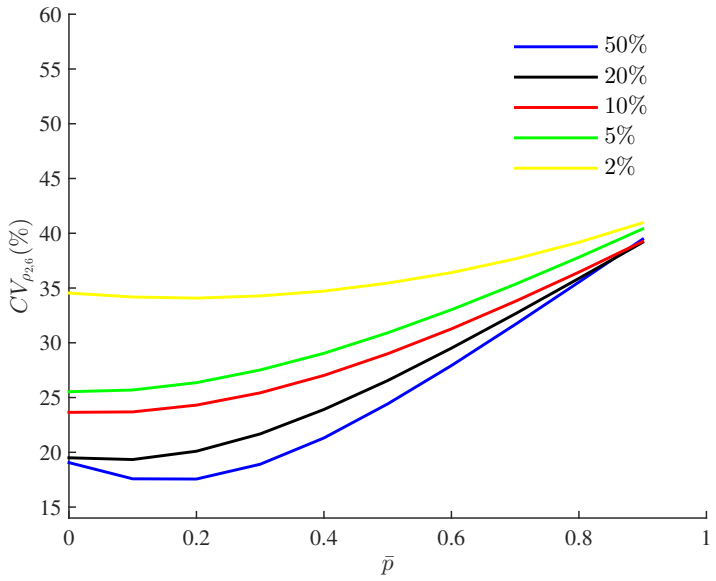

Fig. 15. Performance index (22) that corresponds to the cell in which the on-ramp is located versus percentage of diagonal on-ramp flow, for various penetration rates of connected vehicles, where a moving average, over a horizon of 30 seconds, of the speed measurements is employed.

index for a 5% penetration rate is smaller than the performance index for 10% penetration rate. This may seem contradictory, but it can be explained as follows. In general, from the observed estimated values for the density at the cell where the on-ramp is located, it is evident that for some replications a much larger error in the reported speed from connected vehicles with respect to the real cell speed occurs for the case of 10% than for the case of 5% penetration rates, although on average (among replications) the error is larger for 5%. The deterioration of the performance index for these replications is so significant that causes the performance index to become (slightly) worse for the case of 10% penetration rate.

In addition to this, the estimation performance for the case of 10% penetration rate seems to just happened to be more sensitive to changes of the smoothing factor. This may be attributed to the fact that at such intermediate penetration rates, the available density and lateral flow information from connected vehicles may neither be *sufficiently* rich nor *sufficiently* poor. As a result, the estimation performance may not be *robust* either to a choice of large (in the former case) or small α (in the latter case). Thus, due to the stochastic character of each replication, even a fixed smoothing factor may lead to a different performance index (among replications), which may happen to be toward a worse performance than when just using less information. In other words, it may happen that more available information occasionally deteriorates the performance of the estimation scheme if this information is not as sufficiently good as

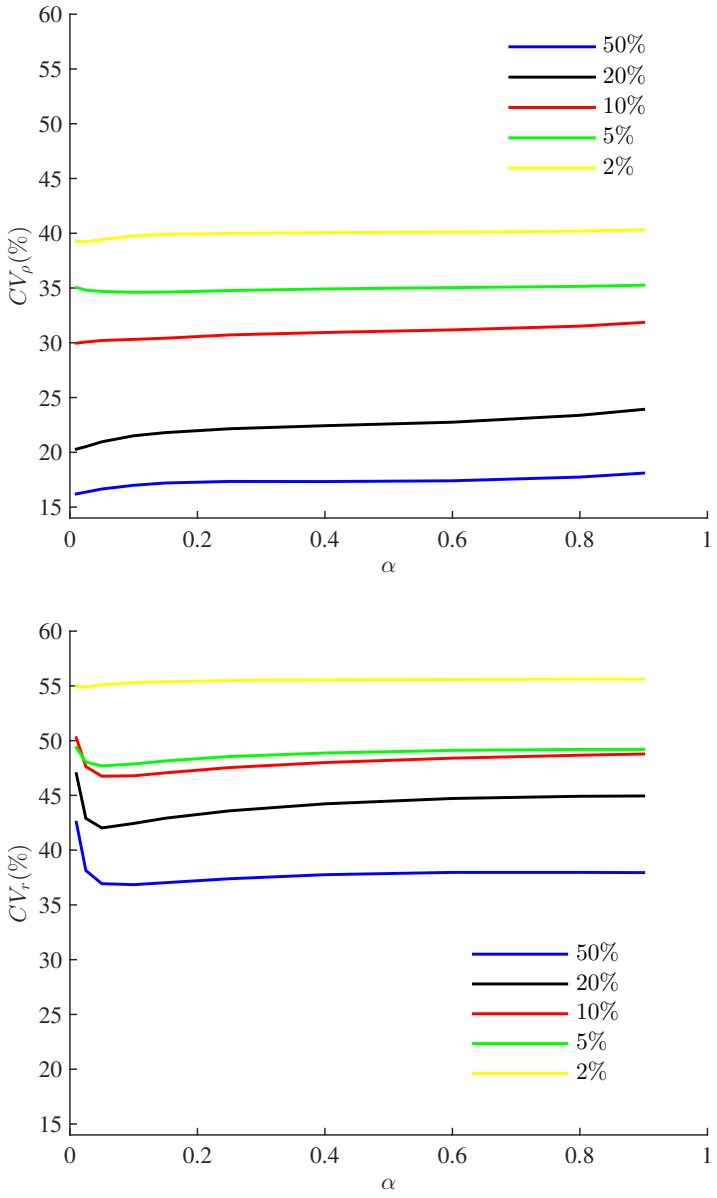

Fig. 16. Top: Performance index (22) versus smoothing factor for various penetration rates of connected vehicles. Bottom: Performance index (23) versus smoothing factor for various penetration rates of connected vehicles.

the estimator may presume.

In Figs. 18 and 19 we show the same results for the case where the speed measurements employed by the estimator are a moving average, over a horizon of 30 seconds, of the speed measurements. As in the case of variations of the percentage $\bar{p}$ shown in Figs. 14 and 15, the picture doesn't change much and the main difference, compared to the case in which the measured speeds are not averaged, lies in the improvement of the estimation performance for low penetration rates.

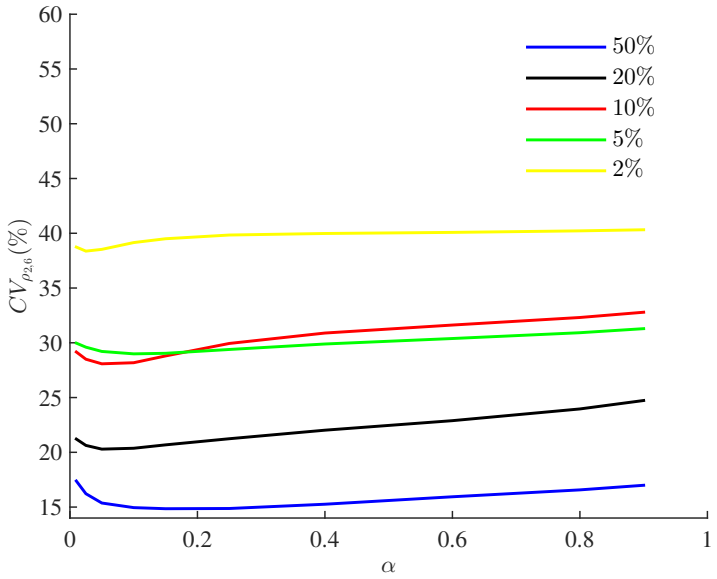

Fig. 17. Performance index (22) that corresponds to the cell in which the on-ramp is located versus smoothing factor for various penetration rates of connected vehicles.

d) Sensitivity of the Estimation Performance to Variations of the Percentages of Diagonal Lateral Flows: In order to confirm our statement that the estimation performance is quite insensitive to variations of the parameters $p_{i,j}$ we show in Figs. 20 and 21 the performance indices for variations of the parameter $p = p_{i,j}$, for all (i, j), with $\bar{p} = 0.3$ and $\alpha = 0.05$ (which corresponds to the baseline case in paragraph *b)* of Section IV-C). Figs. 20 and 21 show that indeed the estimation performance is quite insensitive to variations of the percentages of diagonal lateral flows for almost all penetration rates.

V. Conclusions

We presented a model-based traffic state estimation approach for per-lane density estimation as well as on-ramp flow estimation in highway sections. The developed approach is largely based on the presence of connected vehicles since it mainly employs position, speed, and lane change measurements from connected vehicles. The structural observability properties of the considered highway stretches were studied and necessary as well as sufficient conditions on fixed detectors' configurations, which guarantee the functionality of the estimation scheme, were derived. A discussion on the stability properties of the estimator was also presented. It was also shown, via the utilization of NGSIM real microscopic traffic data, that the performance of the proposed estimation scheme is satisfactory even for low penetration rates of connected vehicles. Finally, it was demonstrated that the developed scheme is insensitive to the model

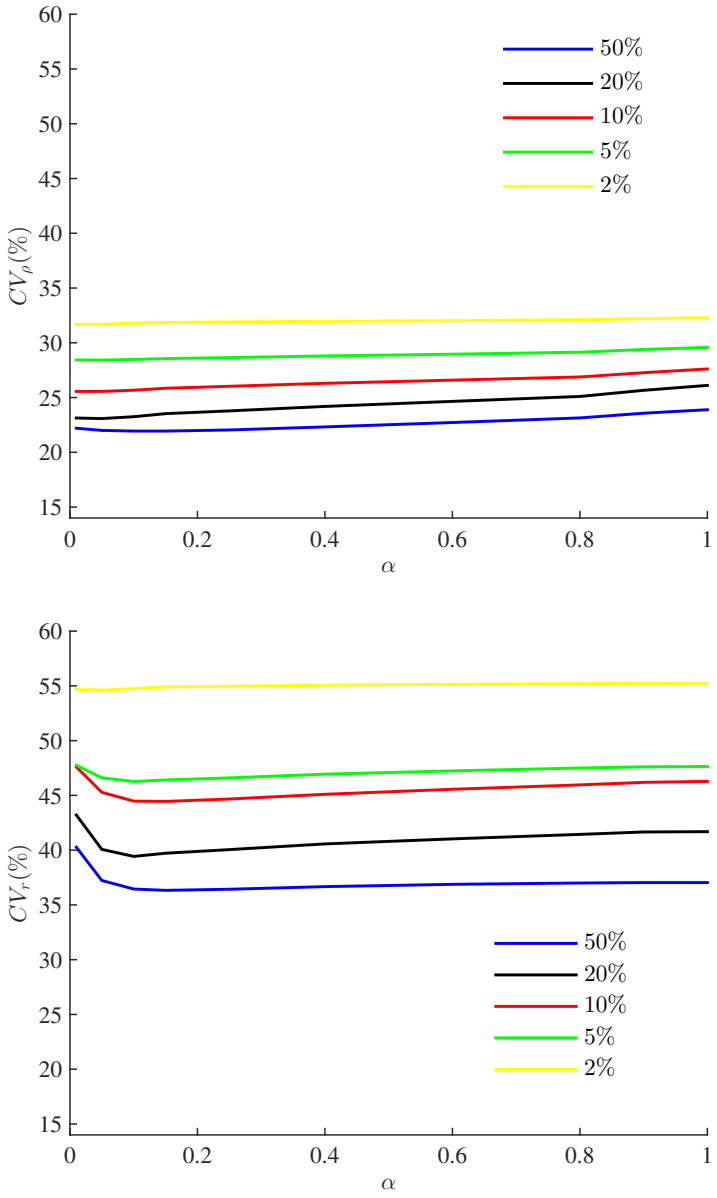

Fig. 18. Top: Performance index (22) versus smoothing factor for various penetration rates of connected vehicles, where a moving average, over a horizon of 30 seconds, of the speed measurements is employed. Bottom: Performance index (23) versus smoothing factor for various penetration rates of connected vehicles, where a moving average, over a horizon of 30 seconds, of the speed measurements is employed.

parameters.

A topic of our ongoing research is the validation of the developed traffic estimation methodology utilizing a microscopic simulation platform, specifically, Aimsun [54].

APPENDIX

a) Condition G_0 from [38]: For every non-empty subset $V \subseteq \{1, \ldots, n\}$ of (state) vertices of $\mathcal{G}\left(\mathcal{A}^{\mathrm{T}}, \mathcal{C}^{\mathrm{T}}\right)$ there exists a vertex $v \in \{1, \ldots, n+r\}$ such that $V \cap \mathrm{Post}\left(\{v\}\right)$ is a singleton.

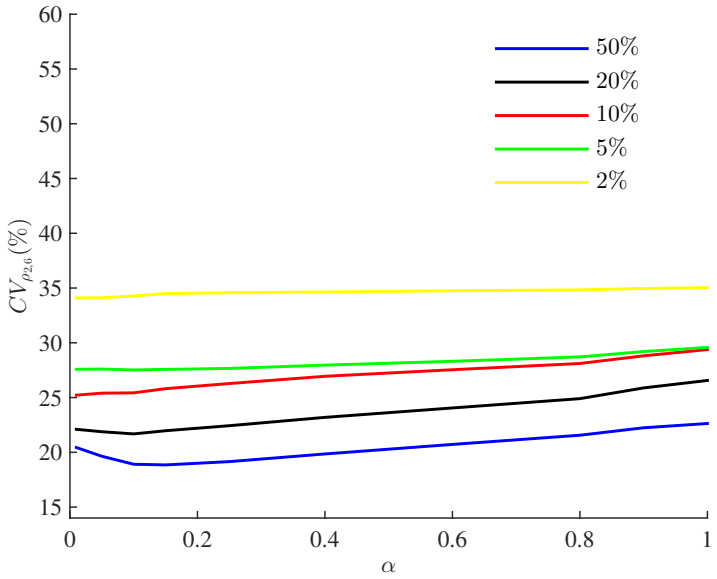

Fig. 19. Performance index (22) that corresponds to the cell in which the on-ramp is located versus smoothing factor for various penetration rates of connected vehicles, where a moving average, over a horizon of 30 seconds, of the speed measurements is employed.

b) Condition G_1 from [38]: For every non-empty subset $V \subseteq \{1, \ldots, n\}$ of (state) vertices of $\mathcal{G}\left(\mathcal{A}^{\mathrm{T}}, \mathcal{C}^{\mathrm{T}}\right)$ that satisfies $V \subseteq \mathrm{Pre}\,(V)$ there exists a vertex $v \in \{1, \ldots, n+r\} \setminus V$ such that $V \cap \mathrm{Post}\,(\{v\})$ is a singleton.

c) Conditions for (Weak) Structural Observability (see, e.g., [25], [27]): A linear system (A, C) is (weakly) structurally observable if and only if: i) The graph $\mathcal{G}\left(\mathcal{A}^{\mathrm{T}}, \mathcal{C}^{\mathrm{T}}\right)$ contains no non-accessible vertex; and ii) the graph $\mathcal{G}\left(\mathcal{A}^{\mathrm{T}}, \mathcal{C}^{\mathrm{T}}\right)$ contains no dilation.

d) Observability Gramian: Consider system (1), (2). The observability Gramian is defined as the matrix $G\left(k_0, k_0 + N^*\right) = \sum_{k=k_0}^{k_0+N^*-1} \theta^{\mathrm{T}}\left(k, k_0\right) C^{\mathrm{T}}(k) C(k) \theta\left(k, k_0\right)$, where θ is defined as $\theta\left(k, k_0\right) = A\left(k-1\right) A\left(k-2\right) \cdots A\left(k_0\right)$, for all $k > k_0$, and it satisfies $\theta\left(k, k\right) = I$, with I denoting the identity matrix.

e) Condition for Observability of Linear Time-Varying Systems (see, e.g., [1]): The pair (A, C) is observable on $[k_0, k_0 + N^*]$ if and only if: $\det\left(G\left(k_0, k_0 + N^*\right)\right) \neq 0$.

f) Specialization to Linear Time-Invariant Systems (see, e.g., [1]): The pair (A, C) is observable if and only if: $\mathrm{rank}\,(O) = n$, where n is the dimension of matrix A and O is the observability matrix defined as $O = \begin{bmatrix} C \\ CA \\ \vdots \\ CA^{n-1} \end{bmatrix}$.

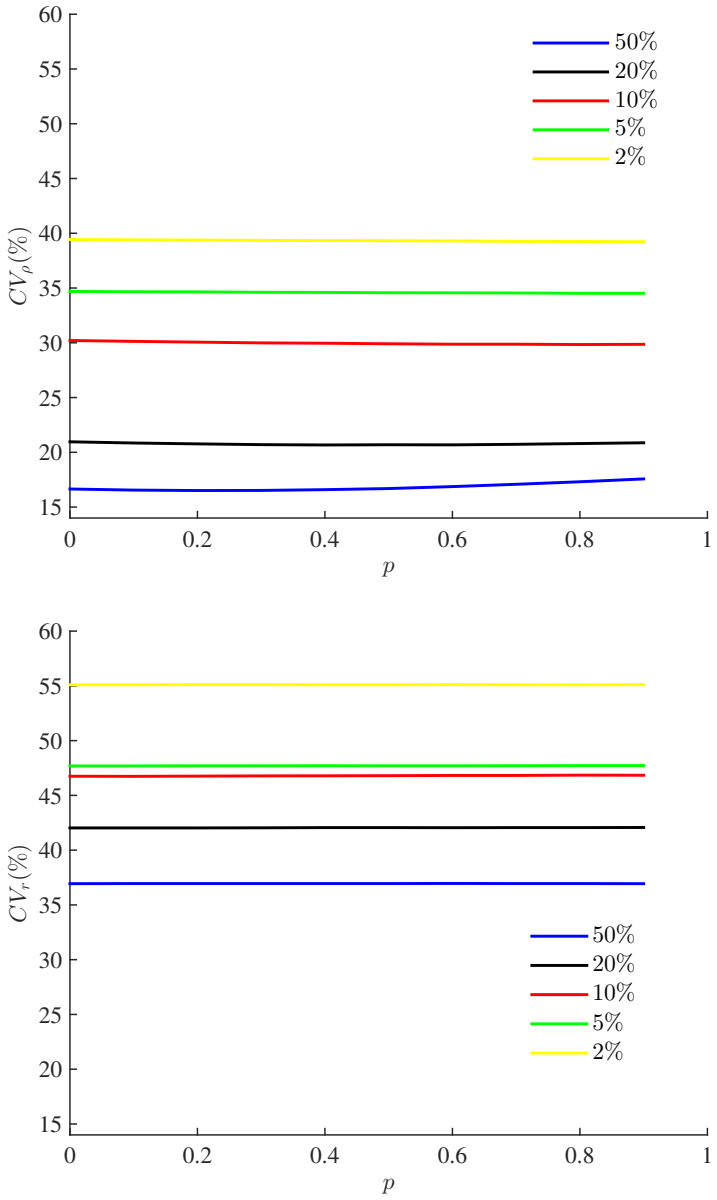

Fig. 20. Top: Performance index (22) versus percentage of diagonal lateral flows for various penetration rates of connected vehicles. Bottom: Performance index (23) versus percentage of diagonal lateral flows for various penetration rates of connected vehicles.

g) Definition of UCO (see, e.g., [30]): The pair (A, C) is UCO if there exist some integer $N^* \geq 1$ and some real $\sigma^* > 0$ such that for all $k_0 \geq 0$ the observability Gramian satisfies $G(k_0, k_0 + N^*) \geq \sigma^* I$.

h) Definition of Uniform Complete Reachability (UCR) (see, e.g., [30]): The pair (A, D) is UCR if there exist some integer $N^* \geq 1$ and some real $\sigma^* > 0$ such that for all $k_0 \geq 0$ the reachability Gramian, defined by $\bar{G}(k_0, k_0 - N^*) = \sum_{k=k_0-N^*}^{k_0} \bar{\theta}(k_0 + 1, k + 1) D(k) D^{\mathrm{T}}(k) \bar{\theta}^{\mathrm{T}}(k_0 + 1, k + 1)$, satisfies $\bar{G}(k_0, k_0 - N^*) \geq \sigma^* I$, where $\bar{\theta}$ is defined as $\bar{\theta}(k_0, k) = A(k_0 - 1) A(k_0 - 2) \cdots A(k)$, for all $k_0 > k$, and it satisfies $\theta(k, k) = I$, with I denoting the identity matrix.

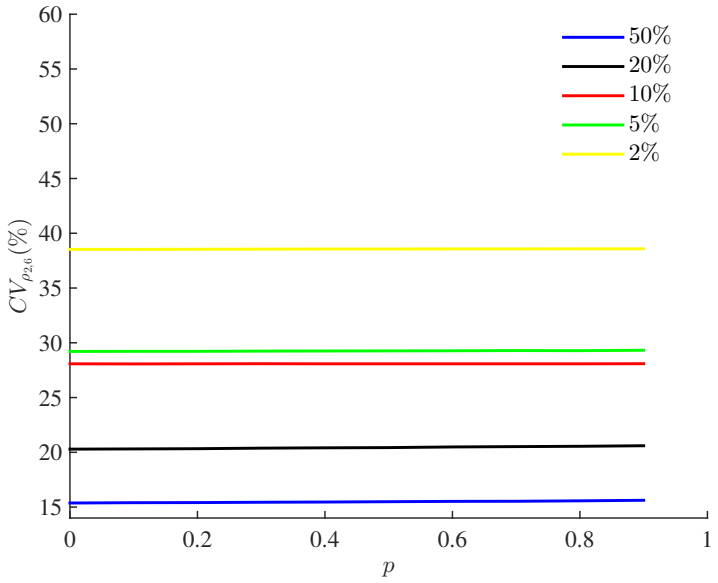

Fig. 21. Performance index (22) that corresponds to the cell in which the on-ramp is located versus percentage of diagonal lateral flows for various penetration rates of connected vehicles.

i) Stability of the Kalman Filter (see, e.g., [30]): Let the matrices A, C, Q, R, and R^{-1} be bounded above and the pair (A, D) UCR for any D such that $DD^{\mathrm{T}} = Q$. Then the Kalman filter (12)–(14) is exponentially stable provided that the pair (A, C) is UCO.

ACKNOWLEDGMENTS

Nikolaos Bekiaris-Liberis was supported by the funding from the European Commission's Horizon 2020 research and innovation programme under the Marie Sklodowska-Curie grant agreement No 747898, project PADECOT.

Claudio Roncoli and Markos Papageorgiou were supported by the funding from the European Research Council under the European Commission's Seventh Framework Programme (FP/2007-2013) / ERC Grant Agreement No. [321132], project TRAMAN21.

REFERENCES

[1] Antsaklis P. and Michel A. N., 2006. Linear Systems, Birkhauser, Boston.

[2] Anand A., Ramadurai G., and Vanajakshi L., 2014. Data fusion-based traffic density estimation and prediction. Journal of Intelligent Transportation Systems 18, 367–378.

[3] Anderson B. D. O. and Moore J.B., 1979. Optimal Filtering, Prentice-Hall, New Jersey.

[4] Baskar L. D., De Schutter B., and Hellendoorn H., 2012. Traffic management for automated highway systems using model-based predictive control. IEEE Transactions on Intelligent Transportation Systems 13, 838–847.

[5] Bekiaris-Liberis N., Roncoli C., and Papageorgiou M., 2016. Highway traffic state estimation with mixed connected and conventional vehicles. IEEE Transactions on Intelligent Transportation Systems 17, 3484–3497.

[6] Chang M. -F. and Gazis D. C., 1975. Traffic density estimation with consideration of lane-changing. Transportation Science 9, 308–320.

[7] Coifman B., 2003. Estimating density and lane inflow on a freeway segment. Transportation Research Part A 37, 689–701.

[8] Courant R., Friedrichs K., and Lewy H., 1928. Uber die partiellen di erenzengleichungen der mathematischen physik. Mathematische Annalen 100, 32–74.

[9] Deng W., Lei H., and Zhou X., 2013. Traffic state estimation and uncertainty quantification based on heterogeneous data sources: A three detector approach. Transportation Research Part B 57, 132–157.

[10] Duret A., Ahn S., and Buisson C., 2012. Lane flow distribution on a three-lane freeway: General features and the effects of traffic controls. Transportation Research Part C 24, 157–167.

[11] Duret A. and Yuan Y., 2017. Traffic state estimation based on Eulerian and Lagrangian observations in a mesoscopic modeling framework. Transportation Research Part B 101, 51–71.

[12] Fountoulakis M., Bekiaris-Liberis N., Roncoli C., Papamichail I., and Papageorgiou M., 2016. Highway traffic state estimation with mixed connected and conventional vehicles: Microscopic simulation-based testing. IEEE Conference on Intelligent Transportation Systems, Rio de Janeiro, Brazil.

[13] Gueriau M., Billot R., El Faouzi N.-E., Hassas S., and Armetta F., 2015. X2V-based information dissemination for highway congestion reduction. Euro Working Group on Transportation (EWGT), Delft, Netherlands.

[14] Hall R. W. and Lotspeich D., 1996. Optimized lane assignment on an automated highway. Transportation Research Part C 4, 211–229.

[15] Hall R. W. and Caliskan C., 1999. Design and evaluation of an automated highway system with optimized lane assignment. Transportation Research Part C 7, 1–15.

[16] Hartung C., Reibig C., and Svaricek F., 2012. Characterization of strong structural controllability of uncertain linear time-varying discrete-time systems. IEEE Conference on Decision and Control, Hawaii, USA.

[17] Herrera J. C. and A. M. Bayen, 2010. Incorporation of Lagrangian measurements in freeway traffic state estimation. Transportation Research Part B 44, 460–481.

[18] Khan S. M., Dey K. C., and Chowdhury M., 2017. Real-Time Traffic State Estimation With Connected Vehicles. IEEE Transactions on Intelligent Transportation Systems 18, 1687–1699.

[19] Kim K., Medanic J. V., and Cho D. I., 2008. Lane assignment problem using a genetic algorithm in the Automated Highway Systems. International Journal of Automotive Technology 9, 353–364.

[20] Knapp C. H., 1973. Traffic density estimation for single and multilane traffic. Transportation Science 7, 75–84.

[21] Knoop V., Duret A., Buisson C., and van Arem B., 2010. Lane distribution of traffic near merging zones influence of variable speed limits. IEEE Conference on Intelligent Transportation Systems, Madeira Island, Portugal.

[22] Laval J. A., Daganzo C. F., 2006. Lane-changing in traffic streams. Transportation Research Part B 40, 251–264.

[23] Lee J. and Park B., 2010. Lane flow distributions on basic segments of freeways under different traffic conditions. Transportation Research Board Annual Meeting, Washington, D.C..

[24] Li P. Y., Horowitz R., Alvarez L., Frankel J., and Robertson A. M., 1997. An automated highway system link layer controller for traffic flow stabilization. Transportation Research Part C 5, 11–37.

[25] Lin C.-T., 1974. Structural controllability. IEEE Transactions on Automatic Control 19, 201–208.

[26] Liu Y.-Y., Slotine J.-J., and Barabasi A.-L., 2011. Controllability of complex networks. Nature 473, 167–173.

[27] Liu Y.-Y., Slotine J.-J., and Barabasi A.-L., 2013. Observability of complex systems. PNAS 110, 2460–2465.

[28] Montanino M. and Punzo V., 2013. Making NGSIM data usable for studies on traffic flow theory. Transportation Research Record 2390, 99–111.

[29] Montanino M. and Punzo V., 2013. Reconstructed NGSIM I80-1. COST ACTION TU0903 -MULTITUDE. available at: www.multitude-project.eu/exchange/101.html.

[30] Moore J. B. and Anderson B. D. O., 1980. Coping with singular transition matrices in estimation and control stability theory. International Journal of Control 31, 571–586.

[31] Papageorgiou M. and Messmer A., 1990. METANET: A macroscopic simulation program for motorway networks. Traffic Engineering & Control 31, 466–470.

[32] Perera M. A. S., Lie B., and Pfeiffer C. F., 2015. Structural observability analysis of large scale systems using Modelica and Python. Modeling, Identification and Control 36, 53–65.

[33] Poljak S., 1990. On the generic dimension of controllable subspaces. IEEE Transactions on Automatic Control 35, 367–369.

[34] Poljak S., 1992. On the gap between the structural controllability of time-varying and time-invariant systems. IEEE Transactions on Automatic Control 37, 1961–1965.

[35] Qiu T. Z., Lu X.-Y., Chow A. H. F., Shladover S. E., 2010. Estimation of freeway traffic density with loop detector and probe vehicle data. Transportation Research Record 2178, 21–29.

[36] Ramaswamy D., Medanic J., Perkins W., and Benekohal R., 1997. Lane assignment on automated highway systems. IEEE Transactions on Vehicular Technology 46, 755–769.

[37] Rao B. and Varaiya P., 1994. Roadside intelligence for flow control in an intelligent vehicle and highway system. Transportation Research Part C 2, 49–72.

[38] Reissig G., Hartung C., and Svaricek F., 2014. Strong structural controllability and observability of linear time-varying systems. IEEE Transactions on Automatic Control 59, 3087–3092.

[39] Rempe F., Franeck P., Fastenrath U., and Bogenberger K., 2016. Online freeway traffic estimation with real floating car data. IEEE Conference on Intelligent Transportation Systems, Rio de Janeiro, Brazil.

[40] Roncoli C., Bekiaris-Liberis N., and Papageorgiou M., 2016. Highway traffic state estimation using speed measurements: Case studies on NGSIM data and highway A20 in the Netherlands. Transportation Research Record 2559, 90–100.

[41] Roncoli C., Bekiaris-Liberis N., and Papageorgiou M., 2016. Optimal lane-changing control at motorway bottlenecks. IEEE Conference on Intelligent Transportation Systems, Rio de Janeiro, Brazil.

[42] Roncoli C., Bekiaris-Liberis N., and Papageorgiou M., 2017. Lane-changing feedback control for efficient lane assignment at motorway bottlenecks. Transportation Research Record 2625, 20–31.

[43] Roncoli C., Papageorgiou M., and Papamichail I., 2015. Traffic flow optimization in presence of vehicle automation and communication systems - Part I: A first-order multi-lane model for motorway traffic. Transportation Research Part C 57, 241–259.

[44] Roncoli C., Papageorgiou M., and Papamichail I., 2015. Traffic flow optimization in presence of vehicle automation and communication systems - Part II: Optimal control for multi-lane motorways. Transportation Research Part C 57, 260–275.

[45] Roncoli C., Papageorgiou M., and Papamichail I., 2016. Hierarchical model predictive control for multi-lane motorways in presence of Vehicle Automation and Communication Systems. Transportation Research Part C 62, 117–132.

[46] Schakel W. J. and van Arem B., 2014. Improving traffic flow efficiency by in-car advice on lane, speed, and headway. IEEE Transactions on Intelligent Transportation Systems 15, 1597–1606.

[47] Schreiter T., van Lint H., Treiber M., and Hoogendoorn S., 2010. Two fast implementations of the adaptive smoothing method used in highway traffic state estimation. IEEE Conference on Intelligent Transportation Systems, Madeira Island, Portugal.

[48] Seo T., Bayen A. M., Kusakabe T., and Asakura Y., 2017. Traffic state estimation on highway: A comprehensive survey. Annual Reviews in Control 43, 128–151.

[49] Seo T. and Kusakabe T., 2015. Probe vehicle-based traffic state estimation method with spacing information and conservation law. Transportation Research Part C 59, 391–403.

[50] Seo T., Kusakabe T., and Asakura Y., 2015. Estimation of flow and density using probe vehicles with spacing measurement equipment. Transportation Research Part C 53, 134–150.

[51] Singh K. and Li B., 2012. Estimation of traffic densities for multilane roadways using a Markov model approach. IEEE Transactions on Industrial Electronics 59, 4369–4376.

[52] Sheu J. -B., 1999. A stochastic modeling approach to dynamic prediction of section-wide inter-lane and intra-lane traffic variables using point detector data. Transportation Research Part A 33, 79–100.

[53] Sun Z., Jin W. L., and Ritchie S. G., 2017. Simultaneous estimation of states and parameters in Newell's simplified kinematic wave model with Eulerian and Lagrangian traffic data. Transportation Research Part B 104, 106–122.

[54] Transport Simulation Systems, 2014. Aimsun & Dynamic Simulators Users' Manual. Transport Simulation Systems.

[55] van Hinsbergen C. P. IJ., Schreiter T., Zuurbier F. S., van LintJ . W. C., and van Zuylen H. J., 2012. Localized extended Kalman filter for scalable real-time traffic state estimation. IEEE Transactions on Intelligent Transportation Systems 13, 385–394.

[56] Varaiya P., 1993. Smart cars on smart roads: problems of control. IEEE Transactions on Automatic Control 38, 195–207.

[57] Wang R., Work D. B., and Sowers R., 2017. Multiple model particle filter for traffic estimation and incident detection. IEEE Transactions on Intelligent Transportation Systems 17, 3461–3470.

[58] Work D. B., Tossavainen O.-P., Blandin S., Bayen A. M., Iwuchukwu T., and Tracton K., 2008. An ensemble Kalman filtering approach to highway traffic estimation using GPS enabled mobile devices. IEEE Conference on Decision and Control, Cancun, Mexico.

[59] Wright M. and Horowitz R., 2016. Fusing loop and GPS probe measurements to estimate freeway density. IEEE Transactions on Intelligent Transportation Systems 17, 3577–3590.

[60] Yuan Y., van Lint J. W. C., Wilson R. E., van Wageningen-Kessels F., and Hoogendoorn S. P., 2012. Real-time Lagrangian traffic state estimator for freeways. IEEE Transactions on Intelligent Transportation Systems 13, 59–70.

[61] Zhang Y. and Ioannou P. A., 2017. Combined variable speed limit and lane change control for highway traffic. IEEE Transactions on Intelligent Transportation Systems 18, 1812–1823.

[62] Zhou Z. and Mirchandani P., 2015. A multi-sensor data fusion framework for real-time multi-lane traffic state estimation. Transportation Research Board Annual Meeting, Washington, DC.